

Deep learning for portfolio optimization

Dzmitry Sei

January 2024

1 Deep learning

In this section basic principles of deep learning will be described. Moreover, we will describe the type of layers used in the thesis.

1.1 General description of NN principles

This subsection will describe general ideas of neural networks in a manner adapted to the context of the master thesis.

All the NNs described in the thesis are implemented using the author's fork of an open-source Python package DeepDow [45]. DeepDow is a deep learning portfolio optimization library, written by Jan Krepl in 2020. The package integrates both stages of the investment process mentioned before. The package can be seen as a combination of auto differentiable convex optimization package CVXPYLAYERS (see later) and code that eases working with financial data. Since the extensive usage of the package, we will describe DeepDow's way of working with NNs.

An NN can be seen as just a function $F : I \rightarrow W$, which transforms input I to the output W .

The output W is a vector of weights, such as $W \in R^{assets}$ and $\sum w_i = 1$. Plus we can set any restriction on w_i that preserves convexity. Suppose we have 5 assets in total, where $asset_1, asset_2, asset_3$ are from the banking sector and assets $asset_4, asset_5$ are from the technological sector. Suppose we don't want to have too big exposure to the banking sector. In this case, we can make our NN not invest more than z fraction of our money (considering both short and long allocation) into this sector by setting the following convex restriction on the output $-z < w_1 + w_2 + w_3 < z$. The set of the restriction, preserving convexity, we can set on the output is very broad [38], which gives us big flexibility for the formulation of investment ideas for our NN.

In the thesis, I is a 3D tensor of asset returns $I \in R^{channels, assets, time}$. The dimensions are:

1. Channel. The dimension containing relevant asset information can be relevant returns, volumes, financial ratios, or any other data. In the thesis, only information about asset returns will be used, so the size of the channel dimension is 1.
2. Time. Controlling the amount of data we are interested in, affecting both past and future. For example, if we are working with past daily data and the dimension is equal to five, this will mean the tensor we have information about the asset for the past five days.

3. Assets. Reflecting the amount of assets we are working with. If we are working with three ETFs, the dimension size is three.

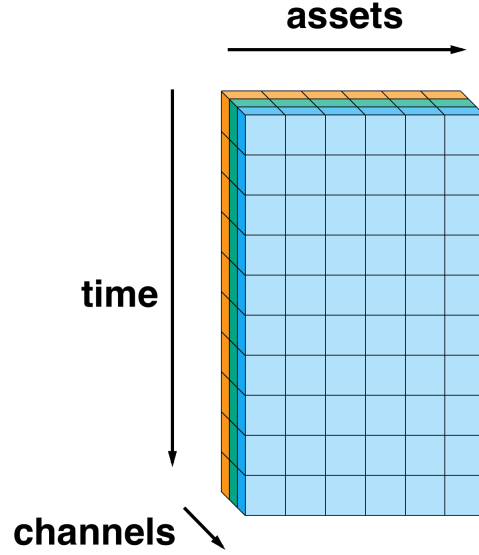


Рис. 1: DeepDow financial data representation [45].

This structure naturally allows us to split any financial data into past, irrelevant immediate future, and useful future as shown in the image below. Irrelevant immediate future can appear in the context of high-frequency portfolio rebalancing, where because of decision-making computational time we had to skip the nearest future. But in the thesis, we are working with daily data, so the time dimension of the immediate future will be zero.

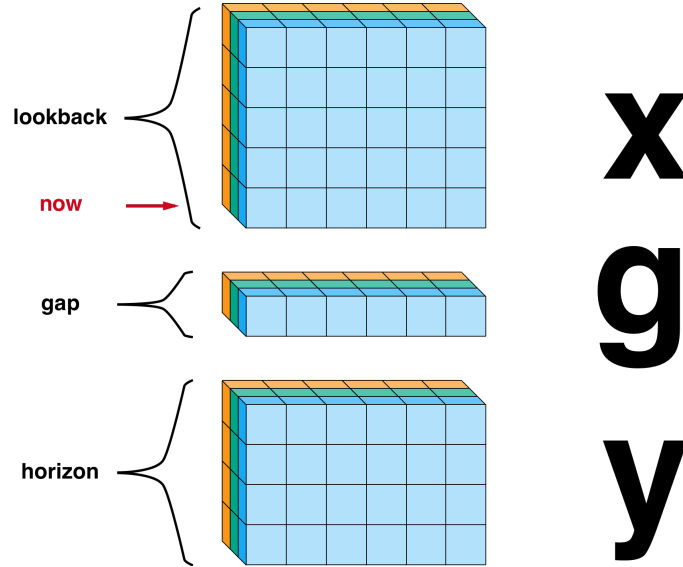


Рис. 2: Time through the eyes of DeepDow [45].

Figure 2 represents how DeepDow is working with time. Initially, tensor x encapsulates all

historical and current knowledge. The second tensor, g , embodies information about the immediate future, which is not accessible for making investment decisions. The last tensor, y , represents the future trajectory of the market.

The amount of data points in the past (x) is controlled by the *lookback* parameter. For example, suppose we are working with daily data and *lookback* = 3; then, we will look only at 3 days in the past. The (useless) immediate future (g) is controlled by the *gap* parameter, for instance, *gap* = 2 implies that the amount of days in the immediate future (g) is two. Similarly, the amount of days we are looking forward into the future (y) is controlled by the *horizon* parameter, following the same logic as for the other parameters.

In the figure below it is shown how this methodology combined with the rolling window principle is working with row data.

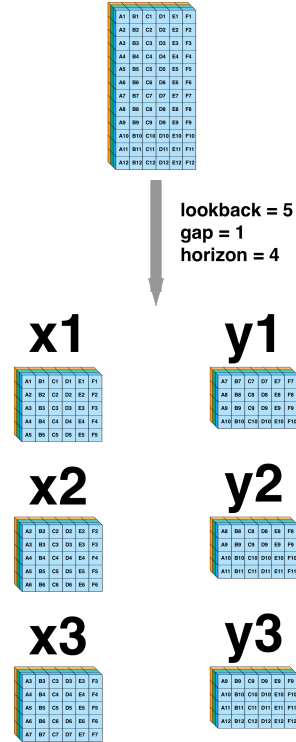


Рис. 3: DeepDow data example [45].

Diving deeply, an NN can be defined as a graph of embedded functions, depending on learnable parameters

$$F(x, \theta) = F_n(x, \theta, F_1, F_2 \dots, F_{n-1}), \quad (1)$$

where θ is a sequence of learnable parameters and F_i is a layer. A layer is just a function, which transforms its input based on a subset of learnable parameters θ_i , such as $\theta_i \in \theta$.

In the simplest case, NN's graph can have a sequential form. In this case, an NN can be expressed in the following way:

$$F(x, \theta) = F_n(F_{n-1}(\dots F_2(F_1(x, \theta_1), \theta_2) \dots, \theta_{n-1}), \theta_n) \quad (2)$$

So in the context of the thesis, NN can be viewed as a function, that transforms a tensor (actually a matrix) of portfolio returns into a vector of weights, as visualized in the figure below.

$$F(\overset{\mathbf{x}}{\text{matrix}}, \theta) = \overset{\mathbf{w}}{\text{vector}}$$

Рис. 4: From returns to portfolio weights based on learned θ [45].

An NN learns θ by minimizing a specific loss function L over the entire (or its subset) dataset used for training.

Suppose we have a training dataset (set of tensors obtained from the initial returns dataset in a way shown in Figure 3) $\{(x_i, y_i)\}_{i=1}^m$. In this case, the goal of the learning phase of our NN F is to solve the following optimization problem:

$$\theta^* = \arg \min_{\theta} \frac{1}{m} \sum_{i=1}^m L(F(x_i; \theta), y_i). \quad (3)$$

where L is a loss function. The exact optimization process and loss functions used will be described later. At this stage it should be noted that loss functions in the thesis are computed in 2 stages:

1. Based on portfolio weights (output of NN $F(x_i, \theta)$) and information about asset returns in future y_i we can compute a vector of portfolio returns in future r_i .
2. The loss function is computed as a scalar function of the vector of portfolio returns r_i .

The whole process is visualized in the figure below.

$$L(\overset{\mathbf{w}}{\text{vector}}, \overset{\mathbf{y}}{\text{matrix}}) = S(\overset{\mathbf{r}}{\text{vector}}) = \text{loss}$$

Рис. 5: Loss function computation process [45].

1.2 Dense layers

1.2.1 General description

We call a layer F_i a dense layer if it transforms an input in the following way:

$$F_i(y, \theta) = \sigma_i(W_i y + b_i), \quad (4)$$

where W_i is layer weights, b_i is layer bias and σ is an activation function [52]. Both W_i and b_i are part of learnable parameters θ .

Activation function σ_i is introduced to allow an NN to deal with nonlinear problems. As we know, the combination of linear functions is a linear function. For example, if we are working with sequential NN, described in Equation 2 with $F_i(y, \theta) = W_i y + b_i$ for all i (σ_i is identity function), the whole NN will be a linear function. In the end, a linear NN is undesirable, because it can't catch complex dependencies in the data (for example can't be used in XOR classification problems [37]).

1.2.2 Activation functions

As mentioned before, in essence, activation functions are just transformers of linear signals into non-linear ones. The set of plausible activation functions is enormous, and a lot of unpublished activation functions performs as well as conventional ones. For example, the unconventional *cos* activation function on the MNIST dataset gives an error rate that is comparable with one of the conventional activation functions [21]. In this section, we will describe only those activation functions among which we will be selecting for constructing our NNs.

In general activation functions are selected from the set of almost everywhere differential functions, which behave like linear, to ease the optimization process.

The most popular activation function is ReLu activation $\sigma(x) = \max(0, x)$ [9]. Note that the function is not differentiable at 0, but this is not the problem because of floating-point arithmetic [20] the probability to get 0 as input of the activation function is almost zero, so this doesn't create a problem in most cases. But if the input is zero we set $\sigma'(0) = 0$ by convention. The second-order derivative of the function is zero, so all the information relevant to optimization is contained in the gradient.

The main drawback of ReLu is the inability to make the parameter updates using gradient in case of non-positive input. To overcome this limitation a lot of generalizations of ReLu were developed, which can find informative gradients everywhere. In the thesis, we are examining Leaky ReLu.

The Leaky ReLU function is defined as follows:

$$f(x) = \begin{cases} x & \text{if } x > 0 \\ \alpha x & \text{if } x \leq 0 \end{cases}$$

Where α is a small constant typically set to a small positive value, often around 0.01.

Compared to the standard ReLU function, which outputs 0 for any non-positive input, Leaky ReLU allows a small, non-zero gradient for non-positive inputs.

The introduction of this small slope for negative inputs helps address the "dying ReLU" problem, which occurs when neurons become inactive during training because they consistently output zero for negative inputs, effectively stopping the gradient flow and hindering the learning process.

By allowing a small gradient for negative inputs, Leaky ReLU helps to alleviate this issue and enables neurons to continue learning, even when the input is negative. This can lead to more robust training and improved performance, especially in deep neural networks where the dying ReLU problem can be prevalent [33].

Another activation function capable of mitigating the dying ReLU problem is the Maxout activation function [22]. Suppose an input to the layer is a $X \in R^d$ vector. Each element X_i of this vector in the context of neural networks is called a neuron.

Maxout considers that each X_i of the dense layer has its own set of learnable weights $\{(W_{ij}, b_{ij})\}$ for $j = 1$ to k

The activation function is defined as follows:

$$\sigma(X)_i = \max(W_{i1}^T x + b_{i1}, W_{i2}^T X + b_{i2}, \dots, W_{ik}^T X + b_{ik})$$

where W_{ij} and b_{ij} represent weight vectors and bias terms specific to neuron i , with k being the number of linear functions considered. Maxout provides the network with the ability to learn an arbitrary convex function, enhancing flexibility and robustness compared to traditional activation functions. However, it should be noted that the increased expressive power of Maxout comes at the cost of higher computational complexity.

1.2.3 Using activation functions for portfolio construction

We can construct an activation function, whose output is a vector, which sums up to 1. So the output can be seen as portfolio weights.

For constructing long-only portfolios we can use the softmax activation function. It is commonly used for classification, but we can treat a Multinoulli output of the activation function as portfolio weights.

The activation function transforms a vector of real-valued scores (logits) into a probability distribution over multiple classes. Mathematically, given an input vector z of length K , the softmax function computes the probability p_i of each class i as follows:

$$p_i = \frac{e^{z_i}}{\sum_{j=1}^K e^{z_j}}$$

where z_i is the i th element of the input vector z . This function ensures that the output probabilities sum up to 1, making it suitable for representing a probability distribution over multiple classes or portfolio weights among several assets.

For incorporating short selling, we can utilize a normalized version of the hyperbolic tangent function (\tanh), which outputs values in the range $(-1, 1)$. Given the same input vector z of length K , the normalized \tanh function transforms each element z_i as follows:

$$t_i = \tanh(z_i)$$

After applying the \tanh function, we normalize the outputs to ensure the sum of their absolute values equals 1, which is suitable for representing portfolio weights including short positions. The normalization can be expressed as:

$$w_i = \frac{t_i}{\sum_{j=1}^K |t_j|}$$

where w_i represents the weight of the i th asset in the portfolio, ensuring that the portfolio weights accommodate both long and short positions with their absolute values summing up to 1.

Dense NN as universal approximator Despite its relative simplicity dense NNs (NNs from Equation 2, with F_i being a dense layer) are a very powerful tool because of the Universal Approximation Theorem.

Consider a simple dense neural network defined by the function

$$y = W_2\sigma(W_1x + b_1) + b_2$$

where

- x is the input vector from R^n ,
- W_1 is the weight matrix connecting the input layer to the hidden layer,
- W_2 is the weight matrix connecting the hidden layer to the output layer, facilitating the mapping to R^m ,
- b_1 and b_2 are the bias vectors for the hidden and output layers, respectively,
- σ denotes the activation function applied element-wise to the hidden layer outputs,
- y is the output vector in R^m ,

The theorem ensures that for any continuous function $g : \mathbb{R}^n \rightarrow \mathbb{R}^m$ and for any $\epsilon > 0$, there exists a configuration of σ , W_1 , W_2 , b_1 , and b_2 such that the neural network F can approximate g with any precision, if hidden layer size will be big enough (amount of rows in W_1 will be big enough)[24].

It was proven that the theorem works for both ReLu and Leak ReLu [30]. Since Maxout can imitate ReLu, this theorem is also applicable to Maxout.

It should be noted that the theorem states the existence of an approximating NN for any continuous function, but doesn't guarantee that it is possible to train an NN respectively. There is no commonly accepted way to find a well-generalizing function from the training set.

Another problem with the theorem is that it doesn't say how big amount of rows in W_1 should be to find a good approximation, but it was shown that increasing the overall amount of layers in dense NN can, in general, reduce the amount of the required neurons (or amount of rows in W_i).

In our context, the theorem can say that if exists a continuous function, which can provide us with optimal portfolio weights, based on asset returns, there is a dense NN, which perfectly approximates it

1.3 Convolutional Layer

1.3.1 Convolution

Convolutional layers have a long history [18] and exist in different forms, in the thesis, the one based on a two-dimensional cross-correlation operation is used.

A convolutional layer can be seen as a function that accepts a two-dimensional matrix as an input and returns a predefined amount of two-dimensional matrixes of the same size as an output. The amount of matrixes returned in a convolutional context is called the amount of output channels.

Given a single-channel (remember that we are using only daily returns channel) input feature map X with dimensions (H_{in}, W_{in}) , and considering a convolutional layer aiming to produce an output with multiple channels (C_{out}) , the operation within the layer for each output channel can be described as follows. For each filter corresponding to an output channel c , where $c \in \{1, 2, \dots, C_{out}\}$, with each filter having dimensions (H_f, W_f) and a bias term b_c , the output Y^c at position (i, j) for channel c is computed by the formula:

$$Y_{ij}^c = b_c + \sum_{m=1}^{H_f} \sum_{n=1}^{W_f} K_{mn}^c X_{i+m, j+n} \quad (5)$$

where:

- Y_{ij}^c represents the intensity of the c -th output feature map at the spatial location (i, j) .
- b_c is the bias associated with the c -th filter.
- K_{mn}^c denotes the weight of the c -th filter at location (m, n) .
- $X_{i+m, j+n}$ is the value of the input feature map at the location $(i + m, j + n)$, implicating the spatial overlap between the filter and the input feature map.

b_c and K_{mn}^c are learnable parameters, which are discovered by an NN during the training process.

This operation is independently applied for each output channel c , allowing the layer to extract and transform multiple features from the single-channel input based on the diverse set of filters K^c .

Note that there is a multichannel version of the described convolutional layer, which can work with a multichannel input.

1.3.2 Pooling

After applying the convolution layer to input matrix X , we obtain an output tensor O of dimension $(C_{out}, H_{out}, W_{out})$. To work further with an output we need to somehow get rid of the channel dimension of the output tensor. There are a lot of aggregating functions, that can deal with the dimension, but in the thesis, we are using average pooling.

Given a tensor O from the convolutional operation with dimensions $(C_{out}, H_{out}, W_{out})$, the average pooling across channels operation is mathematically represented spatial location (i, j) as:

$$\hat{O}_{i,j} = \frac{1}{C_{out}} \sum_{c=1}^{C_{out}} O_{c,i,j}$$

This results in a tensor \hat{O} with dimensions (H_{out}, W_{out}) , where each element is the average of the corresponding spatial location across all output channels.

1.4 Recurrent layers

The layers described before have proved to be useful for a lot of tasks, but they have strong limitations: they assume that data points are independent, and while this is true for many data classes such as images or customer reviews it is not the case about financial returns data [31]. The asset performance at this week is definitely affected by asset performance during the previous week. So we can state the asset performance is not just a sequence of i.i.d. random variables but a stochastic process. It was caught by statisticians more than 70 years ago [39] that for modeling the future state of a process, we should somehow take into account its past state. Recurrent layers can be seen as a natural projection of these ideas on the NN field and can be defined as modified Dense layers, able to take into account states of the network in the past.

1.4.1 The recurrent layers

In the context of recurrent NNs, there is a terminology overlap. There are recurrent layers (networks) as a methodology to work with data taking into account the previous input into the NN. And there is a concrete function also called the recurrent layer. In this section, we will describe the concrete function.

In the thesis recurrent layer (or RNN cell) is a function which at time t updates its hidden state h_t and computes the output o_t at each time step t as follows [3]:

$$h_t = \tanh(W_{ih}x_t + b_{ih} + W_{hh}h_{t-1} + b_{hh})$$

Where:

1. x_t is the input at time t .
2. $h_{(t-1)}$ is the function output at the previous time step $t - 1$ (so-called hidden state), with h_0 being the initial state (in our case $h_0 = 0$).
3. W_{ih} and W_{hh} are the weight matrices for the input and hidden layers, respectively.
4. b_{ih} and b_{hh} are the bias terms for the input and hidden layers, respectively.

This formula encapsulates the core computation within an RNN cell, highlighting the recursive nature of the hidden state computation, which allows the network to maintain and update its "memory" of previous inputs through sequential data processing. The formula is visualized in the image below

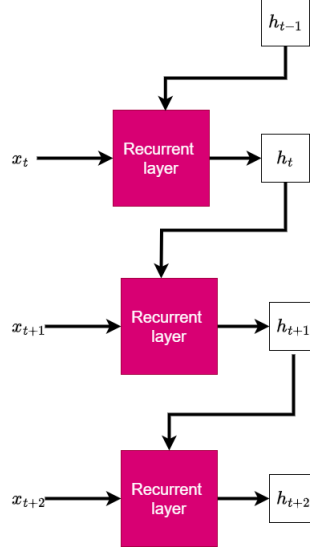


Рис. 6: Recurrent layer.

Note that the formula can be easily extended to include more hidden states (not only h_{t-1} , but h_{t-2} , h_{t-3} and so on), but in the thesis only h_{t-1} is used as a hidden state.

1.4.2 Long Short-Term Memory (LSTM)

Long Short-Term Memory (LSTM) networks are a special kind of Recurrent Neural Network (RNN) capable of learning long-term dependencies, introduced by Hochreiter & Schmidhuber (1997) [23]. They were designed to overcome the limitations of traditional RNNs, particularly the problem of vanishing and exploding gradients [10], making them more effective for a range of tasks where understanding long-term dependencies is crucial (one can easily encounter the problem of vanishing gradients, while trying to train the RNN based NNs proposed by DeepDow [45]). It should be noted that LSTM just reduces the risk of vanishing and exploding gradient but does not fully eliminate it. During the search for the appropriate LSTM-based architectures the author often faced the problem of non-changing training loss, caused by near-zero gradients.

The key innovation of LSTM networks is the introduction of a memory cell c_t , which can maintain its state over time, and three gates (input i_t , forget f_t , and output o_t) that control the flow of information into and out of the cell. The equations governing the LSTM at time t are as follows:

$$f_t = \sigma(W_{xf}x_t + W_{hf}h_{t-1} + b_f) \quad (6)$$

$$i_t = \sigma(W_{xi}x_t + W_{hi}h_{t-1} + b_i) \quad (7)$$

$$o_t = \sigma(W_{xo}x_t + W_{ho}h_{t-1} + b_o) \quad (8)$$

$$\tilde{c}_t = \tanh(W_{xc}x_t + W_{hc}h_{t-1} + b_c) \quad (9)$$

$$c_t = f_t \odot c_{t-1} + i_t \odot \tilde{c}_t \quad (10)$$

$$h_t = o_t \odot \tanh(c_t) \quad (11)$$

Where:

1. x_t ($\dim(x) = d$) is the input at time t .
2. h_{t-1} is the hidden state from the previous time step $t - 1$, with h_0 being the initial state. $\dim(h_i) = h$.
3. c_{t-1} is the memory cell state from the previous time step $t - 1$, with c_0 being the initial state. $\dim(c_i) = h$.
4. W_{x*} and W_{h*} are the weight matrices for the input and previous hidden state, respectively. $\dim(W_{x*}) = (h, d)$, $\dim(W_{h*}) = (h, h)$.
5. b_* are the bias terms, $\dim(b_*) = h$.
6. σ denotes the sigmoid activation function, and \odot denotes element-wise multiplication [40].

This structure allows LSTMs to effectively capture long-term dependencies and decide what information to store, forget, or pass through, making them highly effective for tasks such as language modeling, time series prediction, and sequence generation. The time dependence of an LSTM layer is visualized in the figure below.

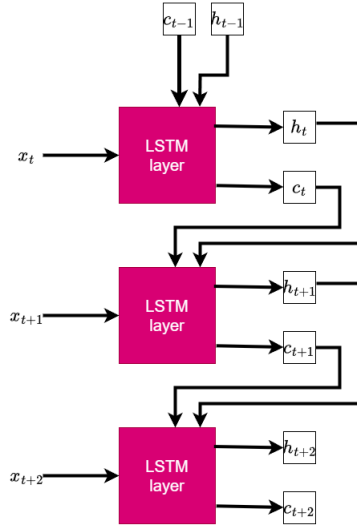


Рис. 7: Time dependence of an LSTM layer.

1.5 Regularization

In this section, we will describe what is regularization in general and specific techniques, that will be used for training NNs utilized for portfolio construction.

1.5.1 General idea

The process of learning for NNs (machine learning algorithms in general) consists of two stages:

1. Choosing learnable parameters θ by minimizing the loss function of other subsets of the entire dataset called training.

2. Estimating the generalization performance of the trained NN by estimating its performance (average loss function for example) over a subset of the initial dataset, called testing. Note for correct estimation testing and training subsets must be disjoint.

The difference between model performance on training and testing set is called generalization gap [52]. The bigger the gap, the lower the ability of our model to generalize well on unseen data. If the gap is too big (determined from the context) we say that the model overfit.

Regularization is a process of manipulating NN architecture aimed at decreasing the generalization gap.

The problems of NNs, if compared with other popular machine learning algorithms, is their expressiveness, ability to perfectly fit (or equivalently to memorize) any training set, and to find structure even in garbage data. For example, it was shown that a specific structure convolutional network, used for image classification, was able to memorize 1.2 million size training data with randomly generated labels [53].

In the context of statistical learning, it is a commonly accepted fact that the more complicated the model the higher its probability of overfitting. But in the context of NNs, it is not always the case. It was shown [34] that under certain conditions increasing NN's model complexity the generalization gap follows the reverse U-shape, being big with small complexity models, big with moderate complexity models, and again small with high complexity problems. Moreover, the ability of NN to generalize is also a nonlinear function of several epochs. An epoch in the context of NN is the number of times the entire dataset is passed forward and backward through the NN. It was shown that after a certain amount of epochs, the generalization gap will increase.

1.5.2 Parameter Loss Penalties

This method aims to limit the magnitude of the learnable parameters θ , thus simplifying the model and helping it to generalize better to unseen data.

Given a loss function $L(F(x_i; \theta))$, where F represents the NN model's prediction for input x_i with parameters θ , regularization can be applied by modifying the loss function to include a penalty term. This results in a new loss function:

$$L_{\text{regularized}}(F(x_i; \theta), y_i) = L(F(x_i; \theta), y_i) + \lambda R(\theta) \quad (12)$$

where:

- $L(F(x_i; \theta), y_i)$ is the original loss function that measures the discrepancy between the NN predictions and the actual target values.
- λ is a regularization parameter that controls the strength of the penalty imposed on the magnitude of the parameters. Choosing an appropriate value for λ is crucial, as too high a value can lead to underfitting, whereas too low a value may not effectively prevent overfitting.
- $R(\theta)$ represents the regularization term. Common choices for $R(\theta)$. The most popular R are $L1$ and $L2$ norms.

It may be optimal to have a specific regularization parameter α for each layer, but the time cost of selecting optimal α is too big to be used in real life. Note it is also commonly used to penalize only a subset of θ .

Although this is a widely used technique in machine learning in general, penalization of the parameter size not always can save the model from overfitting [53].

1.5.3 Early Stopping

It was shown that if data labels have noise, NNs tend to learn correctly labeled data first and then learn the noise [44]. This gives the birth to idea of early stopping: stopping the training process before the NN learns the noise.

Early stopping involves monitoring the model's performance on a validation set at each epoch during training and stopping the training process when the performance on the validation set starts to deteriorate, indicating the beginning of overfitting.

The principle behind early stopping is to use a separate validation dataset that is not used for training the model. The model's performance is evaluated on this validation set at regular intervals during training, typically after each epoch. The process can be summarized as follows:

1. Divide the dataset, used for model training, into two disjoint subsets: training, and validation.
2. During training, monitor the model's performance on the validation set at the end of each epoch (an iteration of training, will be explained later).
3. Continue training as long as the performance on the validation set improves or remains within a certain tolerance.
4. Stop training when the validation performance begins to worsen, indicating that the model is starting to overfit to the training data.
5. Restore the model parameters to the state where the validation performance was at its best.

In the thesis, a modified approach of classical early stopping is used. When the validation performance starts to worsen, we don't immediately stop the training but wait for a certain period, to see if the validation error will improve. The waiting time depends on the specific model used, but on average it is nearly 15.

This technique not only helps in preventing overfitting but also saves computational resources by reducing unnecessary training time.

1.5.4 Dropout

Dropout is a regularization technique that addresses overfitting by temporarily and randomly removing neurons from the neural network during the training process. This method prevents units from co-adapting too much to the data, encouraging the network to learn more generalized representations. The key idea behind dropout is to randomly set a fraction of the input units to 0 at each update during training time, which helps to mimic the effect of training a large number

of neural networks with different architectures in parallel. Dropout can be applied to each layer (except output) of an NN or to a subset of layers.

During training, each neuron (including input neurons but typically not the output neurons) has a probability p of being temporarily "dropped out," meaning it will not contribute to the forward pass and its weight will not be updated during the backward pass. This probability p is a hyperparameter and is set prior to training, with common values ranging from 0.2 to 0.5. The effect of dropout is that the network becomes less sensitive to the specific weights of neurons, leading to a more robust model that is less likely to overfit to the training data.

The dropout procedure can be mathematically represented as follows:

$$r_j^{(l)} \sim \text{Bernoulli}(p) \quad (13)$$

$$\tilde{y}^{(l)} = r^{(l)} * y^{(l)} \quad (14)$$

where $r_j^{(l)}$ is a random variable drawn from a Bernoulli distribution with probability p for each neuron j in layer l , $y^{(l)}$ is the output of neuron j before dropout, and $\tilde{y}^{(l)}$ is the output after applying dropout. The '*' operator denotes element-wise multiplication.

At test time, dropout is not applied; instead, the neuron's output weights are scaled down by a factor equal to the dropout rate p to account for the larger number of active units during testing compared to training. This ensures that the magnitude of the output through any neuron in testing is roughly the same as it would be on average during training [47].

Dropout has been shown to significantly improve the performance of neural networks on a wide variety of tasks by reducing overfitting, leading to models that generalize better to unseen data.

1.5.5 Data augmentation as a proposition of future research

The best way to decrease the generalization gap is to increase the size of the training dataset (ideally we want NN to be trained on all possible data) [21]. But the amount of data we have in real life is limited. The possible solution is to generate synthetic data with similar properties to the original data. For example in the context of image classification different rotations of an image are used to generate several new images, which can be used during the training process.

The problem is that for financial time series, there is no straightforward approach for data generating. But with the development of generative deep learning shortly, we can use generative models like Generative Adversarial Networks (GANs) or Variational Autoencoders (VAEs), which can generate synthetic time series data that is statistically similar to the original dataset. This method can significantly expand the dataset with new, unseen market scenarios, helping models to learn a wider range of patterns.

2 Optimization

As was shown in Equation 1, an NN depends on a set of learnable parameters θ . The goal of the training stage for an NN is to find the set of optimal θ . Optimality was defined in Problem 3.

The purpose of this chapter is to explain the process of searching for optimal parameters (θ by NN.

2.1 How do the NNs learn?

Initially, researchers viewed the process of training a neural network simply as an optimization problem [14]. From mathematical point of view this very untrivial. General shape of a loss function is very tricky, even on simple NNs. Moreover the majority of loss functions are non-convex. An interesting idea for proof of non-convexity of NNs in general is based on the Universal Approximation Theorem introduced in Section 1.2.3. An NN with certain amount of neurons can approximate any function even non-convex with any precision. But we can't approximate non-convex function with convex, so the NN is non-convex [49]. As a result the training process was seen as the process of finding a solution of very tricky generally non-convex problem, which earned NNs a reputation of being unpredictable and unreliable[14].

While approach focused on finding best solution of Problem 3 is natural, it showed not be useful for application. In reality, we don't train NN to find a global minimum of Problem 3, but to find θ , which will allow an NN to be productive on unseen data [52].

It turned out that neural network optimization is very different from standard mathematical optimization. First, it was shown [14] that finding the global minimum of the dataset used for training leads to increasing of generalization error. Another unobvious fact is that for big NNs (and, as will be shown later, NNs implemented in the thesis are relatively big) there is no difference between the performance of local minimums in terms of the loss function on unseen data. This facts makes a painstaking search for the global minimum useless and even harmful.

So in the context of neural networks, optimization is not just about the minimization of a cost function, but is a mixture of mathematics and engineering tricks (for example early stopping described before)[51] aimed to find θ , which can be used for dealing with unseen data.

2.1.1 Stochastic gradient descent and minibatch stochastic gradient descent

As discussed in the previous Section 2.1, while minimizing the loss function a local solution is acceptable, so a simple method as gradient descent is applicable for this task.

The problem with vanilla gradient descent is computational complexity. Given a training dataset $X, Y = \{(x_i, y_i)\}_{i=1}^m$ an NN F , a typical loss function over the entire dataset X, Y is computed as an average of losses of individual points:

$$L(F(X; \theta), Y) = \frac{1}{m} \sum_{i=1}^m L(F(x_i; \theta), y_i)$$

Given that $\nabla_{\theta} L(F(X; \theta), Y) = \frac{1}{m} \sum_{i=1}^m \nabla_{\theta} L(F(x_i; \theta), y_i)$, the computational complexity of each step of gradient descent is $O(m)$ complex. Making the process very ineffective when big datasets are used.

The natural solution to reduce computational complexity is the usage of a subset of X for gradient computation. In extreme cases, only one sample is used. This modification is called SGD.

The algorithm works in the following way[50]. :

1. Shuffle the dataset comprising m observations randomly.

2. Set a value for the learning rate, denoted by η .
3. Initialize the parameters, θ , to start the optimization.
4. For a single data point (x_i, y_i) , update θ as follows: $\theta_{next} = \theta_{current} - \eta \cdot \nabla_{\theta} L(F(x_i; \theta_{current}), y_i)$.
5. Repeat updating θ till a convergence condition is satisfied.

This reduces the optimization step's computational complexity to constant time one $O(1)$.

It should be noted that $\nabla_{\theta} L(F(x_i; \theta), y_i)$ is an unbiased estimator of $\nabla_{\theta} L(F(X; \theta), Y)$:

$$E[\nabla_{\theta} L(F(X; \theta), Y)] = \frac{1}{m} \sum_{i=1}^m E[L(F(x_i; \theta), y_i)] = E[L(F(x_i; \theta), y_i)].$$

The last part of the equation is obtained from classical for NNs analysis assumption that (x_i, y_i) are i.i.d. random variables. However, it should be noted that this assumption is often violated if X represents information about financial asset returns.

The problem of classical SGD is the increased variance of the updates. Suppose we are minimizing $x_1^3 + 2x_2^2$. The function's minimum is point $(0, 0)$. In the figure below the result of default, GD is compared to SGD. The SGD is unstable even after reaching the minimum point.

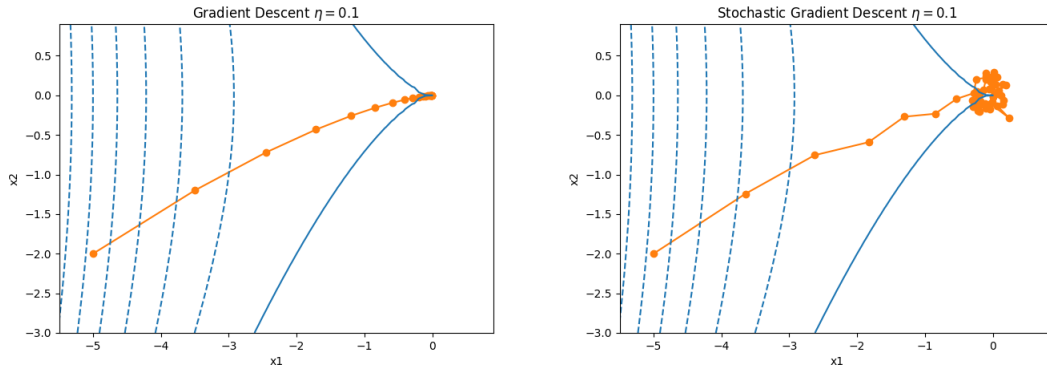


Рис. 8: GD and SGD optimization path.

To make the learning path smoother can make η dynamic, to allow the algorithm gradually reduce the step size. The default approaches for making η dynamics are the following [52]:

1. Exponentially decaying η : $\eta(t) = \eta_0 \cdot e^{-\lambda t}$;
2. Polynomially decaying θ : $\eta(t) = \eta_0 \cdot (\beta t + 1)^{-\alpha}$

The effect of decaying η is shown in the figure below.

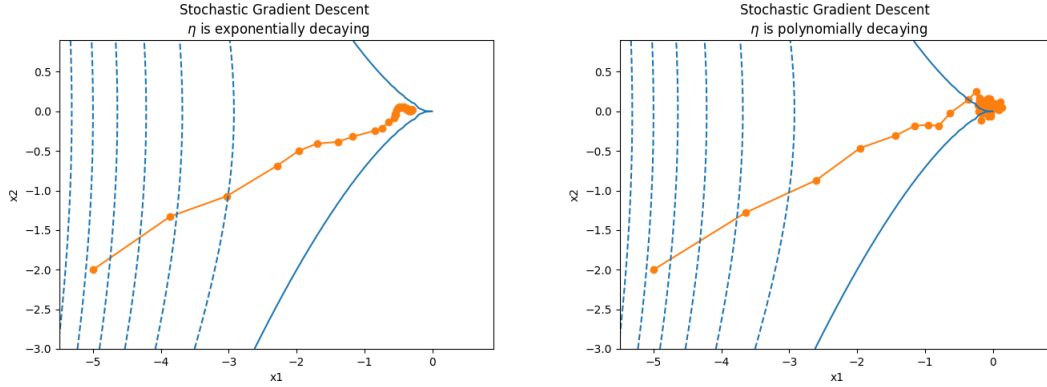


Рис. 9: Decaying η effect.

As we can see, when exponential decay is used, the algorithm does not have time to converge within the given iterations. In both cases the variance is lower than SGD.

In practice pure SGD is rarely used. The first reason is the high variance depicted in the figures above. But also there is a computational problem. Although for complexity of one step of SGD is $O(1)$, if we want to go through the entire dataset of size m , we are still required to perform m steps of vector-to-vector computations.

The solution is to divide the training dataset into batches (subsets of training dataset) and make the iteration over the batches. A step of a GD with batches can be expressed as follows:

$$\theta_{next} = \theta_{current} - \eta \frac{1}{|B_t|} \sum_{i \in B_t} \nabla_{\theta_{current}} L(F(x_i; \theta), y_i),$$

where $B_t = \{(x_i, y_i) \mid i \in \text{batch indexes}\}$ is a batch. The division by $|B_t|$ is reducing variance. Moreover, the bigger batch size, the less optimization steps we need to go through the entire dataset. Selecting the appropriate batch size for training a NN is delicate. On one hand, a larger batch size can lead to faster computation by fully utilizing the parallelism of modern hardware. On the other hand, it can adversely affect the convergence properties of the optimization algorithm. As put by an expert in the field:

Training with large minibatches is bad for your health. More importantly, it's bad for your test error. Friends don't let friends use minibatches larger than 32 [29].

During training of different models (see later) it was noted that batch size 32 is appropriate for use, in our context.

There is also a term mini-batch, which causes ambiguity in the terminology. Some people define mini-batch as subset of training set, and define batch as entire training set[25]. But in PyTorch documentation batch term is used for subset of training set. In the thesis the PyTorch approach is followed. Batch is defined as a subset of training set used for one optimization step. Also the term epoch is used. Epoch is the run of a training algorithm over entire dataset. Suppose we have a dataset consisting from 100 points. If we set batch size equal to 10, this will mean that we will have 10 batches and the one epoch will consist from 10 steps.

2.1.2 Momentum

The problem with GD SGD and batch-based GD is that they work bad when the gradient of the cost functions are disproportional. Suppose we want to minimize

$$0.05x_1^2 + 2x_2^2. \quad (15)$$

The gradient of the function is $0.1x_1 + 4x_2$. The figures below show, the effect of the disproportionality in the gradient. On the

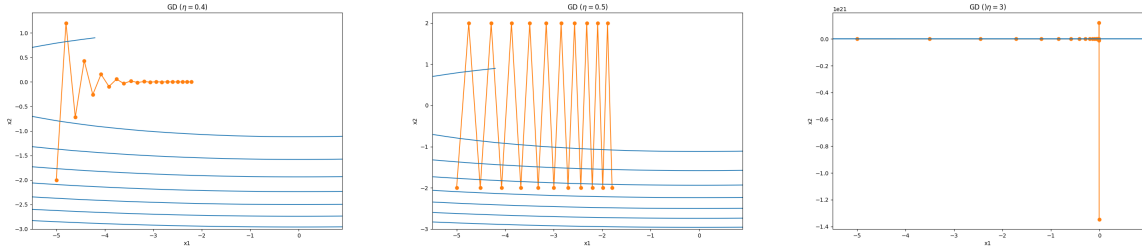


Рис. 10: 20 steps of GD with different η .

As we can see, because of the big effect of x_2 coordinate of the gradient, it is very hard to find the solution for different learning rates η . If η is too small the algorithm is unable to reach the minimum because of the small gradient over x_1 , but when the η is becoming, the step size becoming too big over x_2 dimension, making the optimization path very unstable.

The solution to this problem is to replace gradient in GD step with a weighted sum of gradient at the current point and the sum of the past gradients. Namely, replace $\nabla_{\theta}L(F(X; \theta_t), Y)$ (θ_t is a vector of learnable parameters after t optimization steps) with

$$v_t = \beta v_{t-1} + \nabla_{\theta}L(F(X; \theta_{t-1}), Y),$$

where $\beta \in (0, 1)$ controls the effect of the previous history. After unwinding the recursion we get the following expression [52]:

$$v_t = \beta^2 v_{t-2} + \beta \nabla_{\theta}L(F(X; \theta_{t-2}), Y) + \nabla_{\theta}L(F(X; \theta_{t-1}), Y) = \dots = \sum_{\tau=0}^{t-1} \beta^{\tau} \nabla_{\theta}L(F(X; \theta_{\tau}), Y).$$

When we replace the GD step's gradient with v_t we obtain the so-called momentum GD. Overall the momentum GD step is following:

$$\begin{aligned} v_t &\leftarrow \beta v_{t-1} + \nabla_{\theta}L(F(X; \theta_{t-1}), Y), \\ \theta_t &\leftarrow \theta_{t-1} - \eta v_t. \end{aligned} \quad (16)$$

An interesting analogy can be found among several authors. The process of gradient descent is compared with an individual making their way down a hillside, always opting for the path that slopes most sharply. Momentum is compared with a sphere that rolls along the same decline. The momentum it gathers serves to even out the ride and propel it forward, reducing zigzag motions [19].

The effect of replacing gradient in GD with v_t for the function is shown in the figure below:

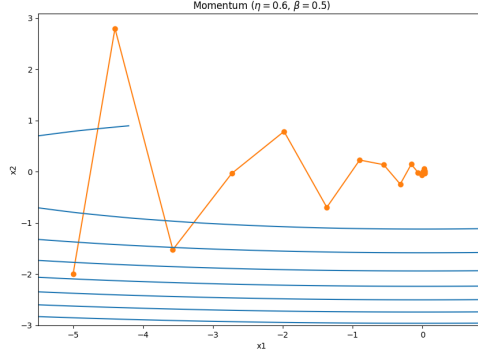


Рис. 11: 20 steps of momentum gradient descent.

As we can see the momentum usage makes the optimization path much more productive.

The momentum idea can be naturally extended on batch gradient descent, we need just to replace the expression for v_t in the following way:

$$v_t = \beta v_{t-1} + \frac{1}{|B_t|} \sum_{i \in B_t} \nabla_{\theta} L(F(x_i; \theta_{current}, y_i)).$$

2.1.3 Root Mean Square Propagation

An alternative way to update default GD to deal with the difficulties of minimizing Cost 15 shown in Figure 2.1.2 is to dynamically update the learning rate η for each coordinate of the gradient.

The most popular algorithm to make the update in this way is RMSProp (Root Mean Square Propagation) introduced by Geoff Hinton in his Neural Networks for Machine Learning course [48] (it was not published, before the introduction during the Coursera video lecture).

The fundamental principle of RMSProp revolves around the modification of the gradient by a running average of its recent magnitude, normalizing the update steps. The mathematical framework of RMSProp is outlined as follows:

$$\begin{aligned} S_t &\leftarrow \gamma S_{t-1} + (1 - \gamma)(\nabla_{\theta} L(F(X; \theta_{t-1}), Y))^2, \\ \theta_{t+1} &\leftarrow \theta_t - \frac{\eta}{\sqrt{S_t} + \epsilon} \odot \nabla_{\theta} L(F(X; \theta_{t-1}), Y). \end{aligned} \tag{17}$$

Where:

- S_t is a vector that holds the exponential moving average of the squared gradients.
- γ is the decay rate, which is a hyperparameter that determines how quickly the influence of the previous squared gradients decays.
- η is a scalar value representing the learning rate.

- ϵ is a small constant added to enhance numerical stability.
- The square operation applied to the gradient $(\nabla_{\theta} L(F(X; \theta_{t-1}), Y))^2$ and the division by the vector $\sqrt{S_t + \epsilon}$ are performed element-wise.
- \odot denotes the element-wise (Hadamard) product.

RMSProp's mechanism of adaptive learning rate adjustments is particularly beneficial in scenarios characterized by noisy or sparse gradients. The effectiveness of RMSProp for minimizing Cost 15 is shown in the figure below.

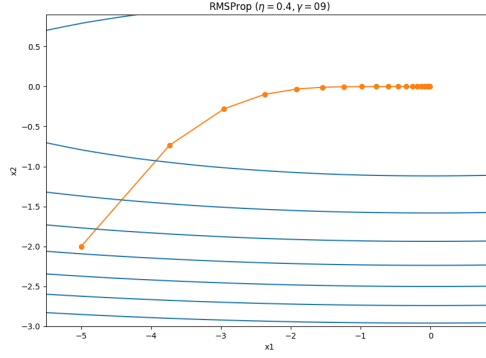


Рис. 12: 20 steps of GD with RMSProp update η .

2.1.4 Two in one, or Adam optimizer

Adam optimizer introduced in 2014 [28] can be seen as a mix of momentum GD ideas described in Section 2.1.2 and RMSProp.

Algorithm 1 Descriptive Caption of Your Algorithm

Require: η (learning rate), β_1, β_2 , θ_0 , $f(\theta) = L(F(X; \theta), Y)$ (objective)

- 1: Initialize: $m_0 \leftarrow 0$ (first moment), $v_0 \leftarrow 0$ (second moment), $\hat{v}_0^{max} \leftarrow 0$
 - 2: **for** $t = 1$ to \dots **do**
 - 3: $g_t \leftarrow \nabla f(\theta_{t-1})$
 - 4: $m_t \leftarrow \beta_1 m_{t-1} + (1 - \beta_1) g_t$
 - 5: $v_t \leftarrow \beta_2 v_{t-1} + (1 - \beta_2) g_t^2$
 - 6: $\hat{m}_t \leftarrow \frac{m_t}{(1 - \beta_1^t)}$
 - 7: $\hat{v}_t \leftarrow \frac{v_t}{(1 - \beta_2^t)}$
 - 8: $\theta_t \leftarrow \theta_{t-1} - \eta \frac{\hat{m}_t}{(\sqrt{\hat{v}_t} + \epsilon)}$
 - 9: **end for**
 - 10: **return** θ_t
-

For the reader, the algorithm should look like a natural continuation of the previously described methods. The only curiosities are \hat{v}_t and \hat{m}_t . The terms $\frac{m_t}{(1 - \beta_1^t)}$ and $\frac{v_t}{(1 - \beta_2^t)}$ in the algorithm serve as bias corrections for the first and second-moment estimates, respectively. Initially, m_t and v_t are

initialized to 0. Because of this initialization and the update rules that are weighted averages, the estimates are biased towards 0 at the start, especially when t is small.

The bias correction terms, $(1 - \beta_1^t)$ and $(1 - \beta_2^t)$, counteract this bias. They adjust the estimates to account for their initialization. Without these corrections, the estimates would be too low at the beginning of training, which can significantly slow down the convergence, especially for high values of β_1 and β_2 .

- For \hat{m}_t , the bias-corrected first moment estimate, the division by $(1 - \beta_1^t)$ increases the value of the moving average estimate, counteracting the initialization bias. As t increases, β_1^t gets closer to 0, reducing the correction impact, which is appropriate since more gradient information has been included over time.
- Similarly, for \hat{v}_t , the bias-corrected second moment estimate, the division by $(1 - \beta_2^t)$ corrects the underestimate of the squared gradients. This is crucial for the adaptive learning rate component, ensuring that it is not too small at the beginning.

By applying these corrections, the algorithm adjusts its steps more accurately, especially during the initial phase, leading to more efficient and reliable convergence.

The difference between Adam performance with and without the corrections for minimizing Function 2.1.2 is shown in the figure below.

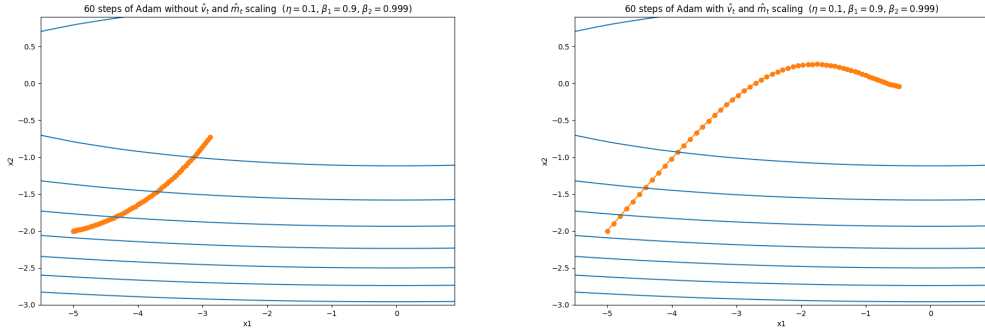


Рис. 13: Performance of Adam with and without the corrections.

As we can see Adam without correction can't even reach the optimum $(0, 0)$ in the given number of steps. The path of the Adam with correction looks very nice, especially when compare with GD path from Figure 2.1.2. The values β_1 and β_2 shown on the figure are default for the optimizer and will use them through the thesis.

Although under certain conditions Adam converges poorly [43]. During experiments on building models (to be described later), the algorithm showed itself to be worthy, and therefore only one was used to train all models.

2.2 Gradients computation

As was shown in the previous section gradient of the loss function $\nabla_{\theta} L(F(X; \theta), y_i)$ is extensively used during the training process.

For automatic computation of gradient in NN extensively used so-called backward propagation. A method used in artificial neural networks to adjust the model's parameters (weights and biases) by propagating the error backward from the output layer to the input layer to minimize the difference between the actual output and the predicted output. This method is based on so-called forward propagation. Forward propagation is just a fancy way to name the prediction process. When based on an NN F , we are doing a prediction $Y = F(X; \theta)$, we are doing forward propagation.

This section will focus on backpropagation for NN consisting from fully connected layers and for NNs containing recurrent layers.

2.2.1 Backpropagation for a fully connected NN

Suppose we are working with a sequential form NN

$$F(x, \theta) = F_n(F_{n-1}(\dots F_2(F_1(x, \theta_1), \theta_2) \dots, \theta_{n-1}), \theta_n)$$

$$F(x, \theta) = F_n(F_{n-1}(\dots F_2(F_1(x, \theta_1), \theta_2) \dots, \theta_{n-1}), \theta_n)$$

with dense layers $F_i(y, \theta) = \sigma_i(W_i y + b_i)$. So $\theta_i = (W_i, b_i)$. Given the loss function

$L(F(X; \theta), Y) = \frac{1}{m} \sum_{i=1}^m L(F(x_i; \theta), y_i)$, our goal is to compute $\frac{\partial L(F(x_i; \theta), y_i)}{\partial W_j}$ and $\frac{\partial L(F(x_i; \theta), y_i)}{\partial b_j}$ for each layer of F (since gradient of sum is sum of gradient the total L is easily computed, if we having losses for the individual points). To ease the notation let's replace $L(F(x_i; \theta), y_i)$ with $l(\theta)$ ((x_i, y_i) is a data point, so is fixed).

A little reminder that each layer F_i is a vector to vector function. Elements of the output vectors are called neurons. Let's define the neuron output a layer i as activation a_i . Since we are discussing sequential architecture for each activation the following equation holds true. $a_i = \sigma(W^i a^{i-1} + b^i)$. To further let's introduce $z_i = W^i a^{i-1} + b^i$, so $a^i = \sigma(z^i)$.

Following notation taken from Nielsen [36] let's define the backpropagation error of neuron i of layer j $\delta_i^j = \frac{\partial l}{\partial z_i^j}$. Intuitively the error δ_i^j measures the sensitivity of the loss to slight perturbation into input to the neuron i of layer j .

Let O be the index of the output layer, we can show, that

$$\delta^O = \nabla_a l \odot \sigma'(z_j^O),$$

where $\sigma'(z_j^O) = \nabla_{z_j} a^j$. The equation can be easily be proved using chain rule $\delta_j^O = \sum_k \frac{\partial l}{\partial a_k^O} \frac{\partial a_k^O}{\partial z_j^O}$, and the fact that $\frac{\partial a_k^O}{\partial z_j^O} = 0$ for $k \neq j$.

We can also prove that

$$\delta^i = ((W^{i+1})^T \delta^{i+1}) \odot \sigma'(z^i). \quad (18)$$

Using chain rule, we can obtain:

$$\delta_j^i = \frac{\partial l}{\partial z_j^i} = \sum_k \frac{\partial l}{\partial z_k^{i+1}} \frac{\partial z_k^{i+1}}{\partial z_j^i}.$$

Now, we consider the weighted input to a neuron in the next layer $i + 1$:

$$z_k^{i+1} = \sum_j w_{kj}^{i+1} a_j^i + b_k^{i+1},$$

which, when applying the activation function σ , becomes:

$$a_k^{i+1} = \sigma(z_k^{i+1}) = \sigma \left(\sum_j w_{kj}^{i+1} \sigma(z_j^i) + b_k^{i+1} \right).$$

Differentiating z_k^{i+1} with respect to z_j^i , we obtain:

$$\frac{\partial z_k^{i+1}}{\partial z_j^i} = w_{kj}^{i+1} \sigma'(z_j^i).$$

Based on this fact, we have:

$$\delta_j^i = \sum_k \frac{\partial l}{\partial z_k^{i+1}} w_{kj}^{i+1} \sigma'(z_j^i).$$

By the definition of matrix multiplication, this can be rewritten as:

$$\delta^i = (w^{i+1})^T \delta^{i+1} \odot \sigma'(z^i).$$

Thus, we have shown the matrix form of backpropagation for the error term δ^i .

For each neuron j of layer i the derivative with respect to bias can be expressed as follows:

$$\frac{\partial l}{\partial b_j^i} = \delta_j^i. \tag{19}$$

This equation can be proved in the following way:

$$\frac{\partial l}{\partial b_j^i} = \sum_k \frac{\partial l}{\partial z_k^{i+1}} \frac{\partial z_k^{i+1}}{\partial b_j^i} = \frac{\partial l}{\partial z_j^{i+1}} \frac{\partial z_j^{i+1}}{\partial b_j^i} = \delta_j^{i+1} \cdot 1$$

In the same way, we can prove, that

$$\frac{\partial l}{\partial w_{jk}^i} = a_k^{i-1} \delta_j^i \tag{20}$$

These ideas are naturally combined with the GD-based optimization algorithms described before. In the pseudocode below you can see how the backpropagation ideas work for training a sequential NN, consisting of dense layers.

Algorithm 2 GD with backpropagation usage for training a neural network [36]

```
1: Input a set of training examples
2: for each training example  $x$  do
3:   Set the corresponding input activation  $a^i(x)$ , and perform the following steps:
4:   Feedforward:
5:   for  $i = 2, 3, \dots, O$  do
6:      $z^i(x) = w^i a^{i-1}(x) + b^i$  and  $a^i(x) = \sigma(z^i(x))$ 
7:   end for
8:   Output error  $\delta^O(x)$ :
9:   Compute the vector  $\delta^O(x) = \nabla_a C \odot \sigma'(z^O(x))$ 
10:  Backpropagate the error:
11:  for  $i = O - 1, O - 2, \dots, 2$  do
12:     $\delta^i(x) = ((w^{i+1})^T \delta^{i+1}(x)) \odot \sigma'(z^i(x))$ 
13:  end for
14:  Gradient descent:
15:  for  $i = L, L - 1, \dots, 2$  do
16:    Update the weights according to the rule  $w^i \leftarrow w^i - \frac{\eta}{m} \sum_x \delta^i(x) (a^{i-1}(x))^T$ 
17:    Update the biases according to the rule  $b^i \leftarrow b^i - \frac{\eta}{m} \sum_x \delta^i(x)$ 
18:  end for
19: end for
```

The algorithm can easily be updated to work with SGD, with mini-batches GD and Adam.

2.3 How to solve a convex optimization problem in a differentiable way?

2.4 Differentiable convex optimization

This subsection will describe the basic principles of CVXPYLAYER, a Python package allowing to creation of differentiable optimization layers.

2.4.1 The need for integrating convex optimization into machine learning process

While discussing NNs activation functions in Section 1.2.2, it was mentioned that we can construct both long-only portfolio and even portfolio allowing shorting using just specific activation functions, as was done in [54]. But the problem with this approach is that it is very restrictive. Yes, we can make an NN return a vector, which sum up to one and call the result portfolio. But imposing further restrictions is very hard. Suppose we can find a numerical trick, allowing to restrict the maximum allocation to a single asset or even to a sector. But, in the case we will need to change the restrictions or to introduce new, we will have to spent time again on thinking about the way of implementing the restrictions. The solution is to somehow insert an ability to solve optimization problem with given set of restrictions into an NN, which is more expressive than anything we can get by chaining different numerical operations together. This solution is a differentiable convex optimization layer.

2.4.2 CVXPY as the basis for formulating optimization problems

CVXPY is a Python framework that allows to solve of parameterized convex optimization problems. Understanding it's principles is crucial for understanding CVXPY LAYER, because CVXPY LAYER is based on the ideas of CVXPY, and directly uses the main concepts. The goal of this section is to briefly describe this principles.

A classical convex optimization problem is an optimization problem with a convex objective, convex inequality constraint, and affine equality constraint which can be expressed in the following format:

$$\begin{aligned} & \underset{x}{\text{minimize}} && f_0(x) \\ & \text{subject to} && f_i(x) \leq 0, \quad i = 1, \dots, m_1, \\ & && g_i(x) = 0, \quad i = 1, \dots, m_2, \end{aligned} \tag{21}$$

where $x \in \mathbb{R}^n$, $f_i : \mathbb{R}^n \rightarrow \mathbb{R}$ are convex, and the functions $g_i : \mathbb{R}^n \rightarrow \mathbb{R}$ are affine.

CVXPY is the next evolutionary step after CVX [17], which allowed to solve problems, which follows the above definition. The main functional feature is the introduction of parameters. Besides solving the original Problem 21, CVXPY also able to solve parametrized convex optimization problem:

$$\begin{aligned} & && f_0(x; \theta) \\ & \text{subject to} && f_i(x; \theta) \leq 0, \quad i = 1, \dots, m_1, \\ & && g_i(x; \theta) = 0, \quad i = 1, \dots, m_2, \end{aligned} \tag{22}$$

where $\theta \in \mathbb{R}^p$ is a vector of parameters, controlling the form of the optimization problem, and f_i and g_i have the same curvature properties as in the 21.

Initially, this idea may seem insignificant, but in fact, it lies at the core of differentiable convex optimization. Solution of Problem 22 can be viewed as a function, which maps the parameter θ to the minimum:

$$\begin{aligned} x^*(\theta) &= \underset{x}{\operatorname{argmin}} f_0(x; \theta) \\ & \text{subject to} \\ & f_i(x; \theta) \leq 0, \quad i = 1, \dots, m \\ & A(\theta)x = b(\theta) \end{aligned}$$

This allows us to define the derivative of the optimization problem x_* with respect to θ . Finding this derivative is the goal of differentiable optimization layers.

The optimization problems that fall under the definitions, shown above, can be classified as: linear programs (LP), quadratic programs (QP), second-order cone programs (SOCP), semidefinite programs (SDP), cone programs (CP), graph form programs (GFP). Between the classes there is a hierarchy: every LP can be expressed as QP, every QP can be expressed as SOCP, every SOCP to SDP, every SDP to CP, every CP to GFP [5]. Since CVXPY mainly focus on the classes up to GFP (excluding), we will ignore this class in further discussion. The hierarchy of the relevant classes is depicted in the figure below.

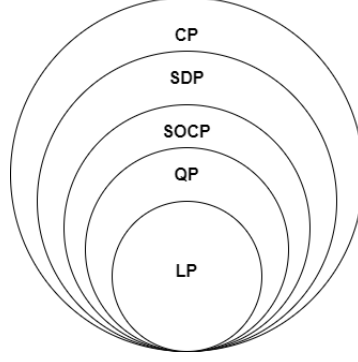


Рис. 14: Hierarchy of convex problems. Drawn based on ECCV2020 tutorial [7].

In general, CVXPY can solve any problem from any class up to CP. The approach used by CVXPY can be described in the following way: transform the original optimization problem into a standard form cone program equivalent to the original one, solve the obtained problem, and obtain the solution of the original problem from the solution of the cone program. Namely, CVXPY see each parametrized convex optimization problem (like Problem 22) $x_*(\theta)$ as composition:

$$x_* = R \circ s \circ C, \quad (23)$$

where

- C maps the encoded Problem 22 and θ to standard form of specific problem (it can be LP, QP or any other),
- s solves the obtained standard form problem to obtain solution \tilde{x}_* of the cone problem,
- R is the retriever, which maps the solution of the standard form problem to the solution of the original problem x_* [4].

CVXPY provides the user with ability to encode Problem 22 in Python-based domain-specific language (DSL) allowing high-level formulation of optimization problems.

An example of an expression of an optimization problem in the DSL is shown below:

Листинг 1: DSL representation of the problem

```
import cvxpy as cp

w = cp.Variable(n_assets)

# Define the risk as the portfolio variance
risk = cp.sum_squares(self.covmat_param_sqrt @ w)
# Optimization problem to minimize the risk (portfolio variance)
# subject to weights summing to 1
# and each weight being bounded [-max_weight, max_weight]
prob = cp.Problem(cp.Minimize(risk),
                  [cp.sum(w) == 1, w <= max_weight, -w <= max_weight])
```

The DSL provided by CVXPY is very expressive but must follow a ruleset called disciplined convex programming (DCP) [8]. DCP employs a set of predefined elementary functions (such as

cp.sum_squares from the listing above), termed atoms, with established curvature properties (affine, convex, or concave) and designated monotonicities for each argument. The DCP allows to combine atom in specific way to check the curvutare of the final expression. The combination is done based on connvex composition theorem, that allows for the combination of functions, termed as atoms, under certain conditions to maintain convexity. Specifically, let's consider a convex function that is non-decreasing in one subset of arguments and non-increasing in another. When this function is composed with other functions that are convex in the non-decreasing arguments, concave in the non-increasing arguments, and linear otherwise, the resulting composite function is also convex. This principle ensures the preservation of convexity under composition, provided the individual functions comply with these monotonicity and curvature conditions [4].

Based on DSL CVXPY is building an expression tree, representing the optimization problem, allowing to analysis information about curvutare conditions, check if the problem follows DCP and obtain and intermediate representation of the problem. A tree is build for each f_i and g_i of Problem 22.

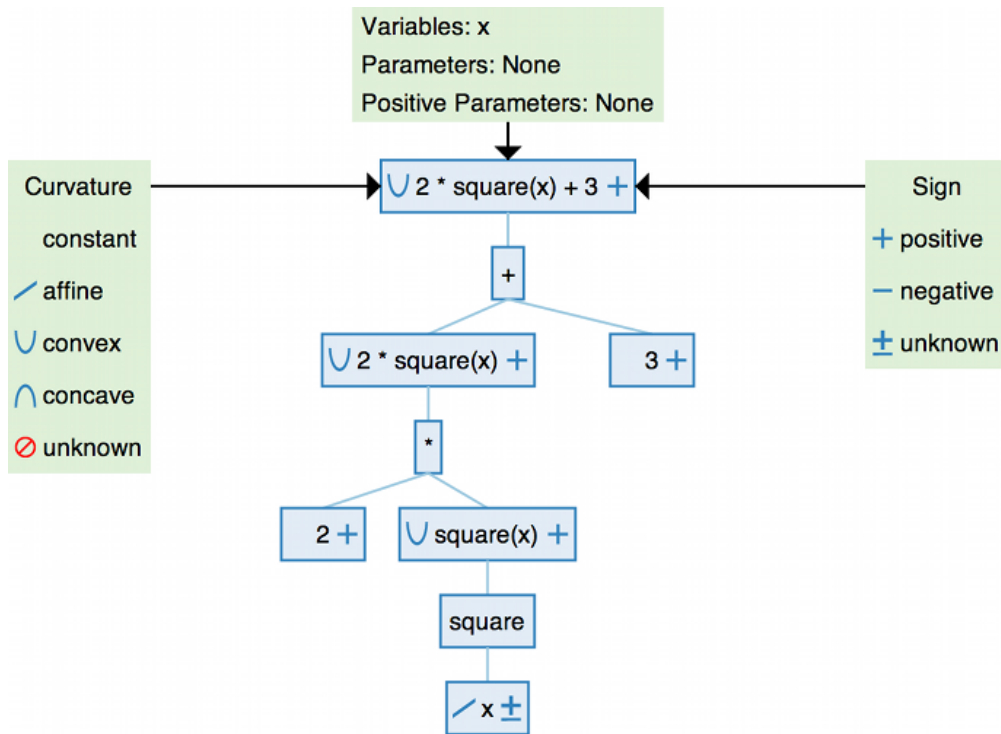


Рис. 15: Example of expression tree, built by CVXPY. This image is sourced from the CVXPY documentation [8], used under the Apache License 2.0. www.apache.org/licenses/LICENSE-2.0.

After building the trees the problem is analyzed to find parameters of standard form problem . After analyzing the problem is matched to a relevant solver. Solver is a program with a low-level interface designed to solve specific optimization problems. The whole architecture of CVXPY is shown in the figure below.

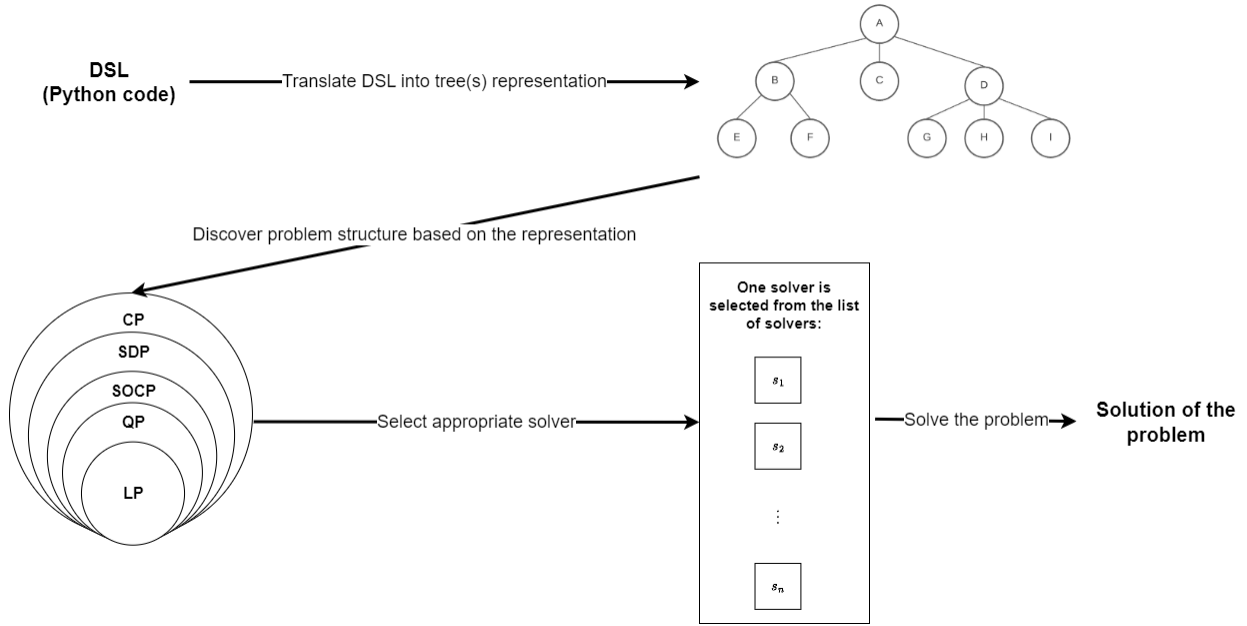


Рис. 16: CVXPY architecture. Drawn based on ECCV2020 tutorial [7].

2.4.3 Solving convex the problems in a differentiable way

CVXPYLAYER is updated version of CVXPY allowing to compute derivative of the solution of a parametrized convex optimization problem with respect to parameters θ .

The main architectural difference from CVXPY is that all the problems are mapped to cone program. And only one solver is used: the solver for a cone program. So in CVXPYLAYER a DSL is transformed into tree, tree is transformed into cone problem, the problem is solved by specified solver. The flow is shown in the figure below.

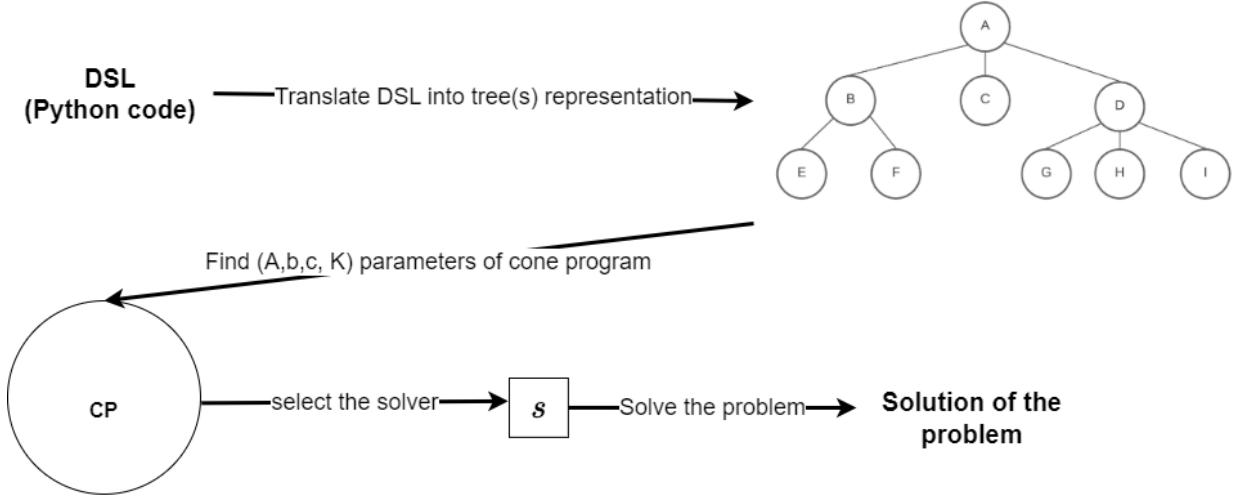


FIG. 17: DSL flow of CVXPYLAYERS. Drawn based on ECCV2020 tutorial [7].

Given high position of CP in convex optimization hierarchy, shown in Figure 2.4.2, the fact of mapping to CP is not restrictive.

A cone program can be seen as a universalization of linear programs [35] of the following form:

$$\begin{aligned} & \text{minimize} && \mathbf{c}^T \mathbf{x} \\ & \text{subject to} && \mathbf{b} - \mathbf{A}\mathbf{x} \in \mathcal{K}, \end{aligned} \tag{24}$$

where the set $\mathcal{K} \subseteq \mathbb{R}^m$ is a nonempty, convex cone, and the problem data are $\mathbf{A} \in \mathbb{R}^{m \times n}$, $\mathbf{b} \in \mathbb{R}^m$, and $\mathbf{c} \in \mathbb{R}^n$.

Below you can see an example of manual canonization of an optimization problem, in the form that is relevant to the thesis. Suppose $\mathbf{Q} \in \mathbb{R}^{2 \times 2}$ and $w \in \mathbb{R}^2$. The optimization problem is:

$$\begin{aligned} \min_w & \quad \|\mathbf{Q}w\|_2 \\ \text{s.t.} & \quad \mathbf{1}^\top w = 1, \\ & \quad -1 \leq w_i \leq 1. \end{aligned}$$

This is equivalent to:

$$\begin{aligned} \min_t & \quad t \\ \text{s.t.} & \quad (t, w_1, w_2) \in \mathbb{J}, \\ & \quad \mathbf{1}^\top w = 1, \\ & \quad -1 \leq w_i \leq 1, \end{aligned}$$

where $\mathbb{J} = \{(t, w_1, w_2) \mid \|Qw\|_2 < t\}$ is a convex cone. The problem is a cone problem with:

$$\begin{aligned} x &= \begin{bmatrix} t & w_1 & w_2 \end{bmatrix}^T, \\ c &= \begin{bmatrix} 1 & 0 & 0 \end{bmatrix}^T, \\ b &= \begin{bmatrix} 0 & 0 & 0 & 0 & 0 & 0 & 0 & 0 \end{bmatrix}^T, \\ \mathcal{K} &= \mathbb{J} \times \{1\} \times \mathbb{R}_{[-1, \infty]} \times \mathbb{R}_{[-1, \infty]} \times \mathbb{R}_{[-1, \infty]} \times \mathbb{R}_{[-1, \infty]} \\ -\mathbf{A} &= \begin{bmatrix} 1 & 0 & 0 \\ 0 & Q_{11} & Q_{12} \\ 0 & Q_{21} & Q_{22} \\ 0 & 1 & 1 \\ 0 & 0 & -1 \\ 0 & -1 & 0 \\ 0 & 1 & 0 \\ 0 & 0 & 1 \end{bmatrix}. \end{aligned}$$

This was an example of manual canonization. Both CVXPY and CVXPYLAYERS do it automatically.

For CXPYLAYERS, give the equation 23, C is a map from DSL and θ to cone problem parmaters (A, b, c) , s is the solver of the cone problem and R maps the solution of the cone \tilde{x}_* problem to the solution of the original x_* . This looks in the following way:

$$x_*(\theta) = R(s(C(\theta))) = R(s(A, b, c)) = R(\tilde{x}_*)$$

$\frac{dx}{d\theta}$ is computed using chain rule.

To make the differentiation of x_* effective CVXPYLAYERS restrict itself only to the problems for which C and R in 23 are affine. This is so-called affine-solver-affine (ASA) format. To ensure that a problem x_* is in ASA format CVXPYLAYERS introduce so called disciplined parametrized programming (DPP), a ruleset being a subclass of DCP. Each DPP problem is DCP, but not vice versa. The problems are formulated using the same Python-based DSL.

The problem with DCP is that it fully recreate the process of construct C if θ is changed. This is crucial for the thesis topic, because in the thesis CVXPYLAYERS is used for NNs construction. As you will see the number of passes through the entire dataset (epochs) in the implemented NNs can exceed 100. Given the dataset size bigger than 3000 datapoints, and for each data point different θ will be used, the amount of C computation is bigger than 300000, which is computationally expensive. This kill all the benefits of using specific solver for narrower problem (using LP specific solver for LP problem is often much faster than using CP solver for LP problem). DPP allows to cache C , allowing it fast reusing [15].

DPP rules are simple, but their understanding requires understanding of DCP, and it is better to consult documentation [8] for fully understanding the grammatics. For the topic of the thesis only the following example is important. Assume matrix $A \in \mathbb{R}^{m \times m}$ denotes a (symmetric) positive semidefinite matrix, and vector $v \in \mathbb{R}^m$ is a variable. The quadratic form $v^\top A v$ is not DCP-compliant. But the form can be equivalently expressed as $\|A^{1/2}v\|_2^2$, with $A^{1/2}$ being a new parameter that squares to A .

As mentioned before the DPP optimization problem allows caching. The caching can be easily implemented using the following theorem.

For a optimization task, which follows DPP, C can be expressed using a sparse matrix $Q \in \mathbb{R}^{n \times (p+1)}$ and a sparse tensor $R \in \mathbb{R}^{m \times n \times (p+1) \times (p+1)}$, with m indicating the number of constraints involved. By defining $\hat{\theta} \in \mathbb{R}^{p+1}$ as the merged entity of θ and a unitary scalar, the essential elements of the problem can be represented. Here, c is derived as $c = Q\hat{\theta}$ and the matrix-vector pair $[A \ b]$ is constructed from the sum $\sum_{i=1}^{p+1} R_{:::,i}\hat{\theta}_i$ [4].

So if we store, Q and R in cache, we can quickly compute $C(\theta)$ using just matrix computation.

3 Trained models

This section will describe how the NN models were trained, their architecture, and insights gained from training.

3.1 Description of training process

As a loss function, a minus (we want to minimize the loss function) Sharpe Ratio was selected. For an NN F , dataset $(X, Y) = \{(x_i, y_i) \mid i = 1, \dots, m\}$ (as a reminder, y_i is a 2D matrix with columns mean asset returns, representing a time point in the future), and learned parameters θ , a loss function looks in the following way:

$$L(F(X; \theta), Y) = \sum_{i=1}^m L(F(x_i, \theta), y_i) = \sum_{i=1}^m L(w_i, y_i) = \sum_{i=1}^m -\frac{\hat{E}(y_i w_i)}{\hat{\sigma}(y_i w_i)},$$

where $y_i w_i$ is multiplication of matrix of future asset returns y_i and vector of weights w_i , \hat{E} is sample mean and $\hat{\sigma}$ is sample standard deviation.

As mentioned in the introduction we want to assess the ability of NN-based models to learn in different data environments. That is why two time periods were used for the experiments:

1. (2007,1,3)-(2020,12,15). In the thesis, we call this period Period A. In this period a subperiod (2007,1,3)-(2017,12,15) is used for training the original model. The remaining years are used for backtesting
2. (2007,1,3)-(2023,12,15). We call this period Period. By analogy, (2007,1,3)-(2020,12,15) is used for training (2020,12,15)-(2023-12,15) is used for backtest.

To set up NN architecture, we are supposed to use hyperparameters. Hyperparameters are non-trainable parameters of an NN, which are selected before the training process starts such as type of activation function, amount of layers, optimizer, regularization techniques, and so on.

To select hyperparameters, the hold-out validation method was utilized. Specifically, the original training dataset was divided into a training subset and a validation subset, with proportions of 80% for training and 20% for validation [42]. The division is visualized in the figure below.

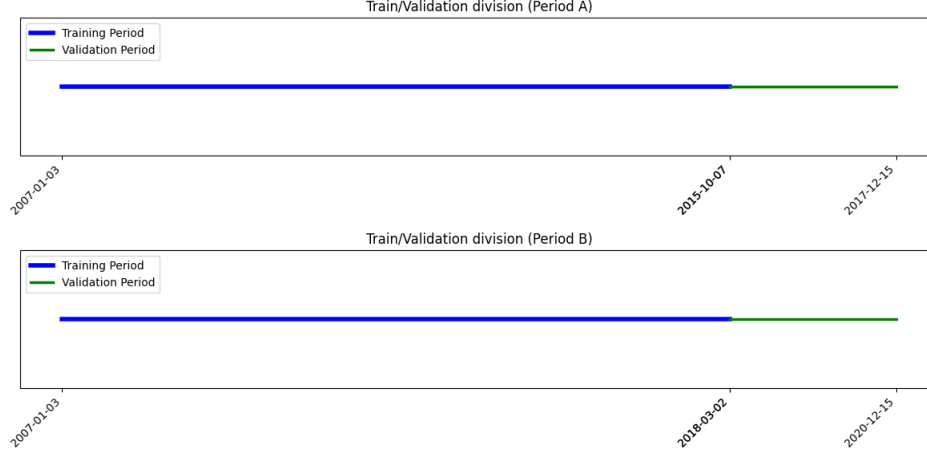


FIG. 18: Train/validation division of the subset used for training.

For each proposed set of hyperparameters, a model was trained on the training data. The performance of each trained model was then recorded on the validation set. The set of hyperparameters was selected based on achieving the best performance on the validation set.

There is a popular alternative to the hold-out validation method, known as *k-fold cross-validation*. The core idea of this method is to divide the original training dataset into k disjoint subsets (or "folds"). The model is then trained and validated k times, with each iteration using a different fold as the validation set and the remaining $k - 1$ folds combined as the training set. The model's performance is assessed by taking the average of the performance metrics across all k iterations. This approach ensures that every data point is used for both training and validation exactly once, providing a comprehensive evaluation of the model's performance [6].

However, training neural networks is time-consuming, and the k -fold cross-validation process can significantly increase the computational burden because it requires training k separate models. Due to the time demands of both neural network training and the cross-validation process itself, it was decided to utilize the hold-out validation method.

As the core optimization technique in the thesis batch-based Adam optimizer is used. Adam optimizer is a local optimizer (and it is completely okay to have find a local minimum of loss function in the context of NN, as was shown before). NN's loss surface can be very nonconvex and the problem with local optimizers is that they can stuck in a local hollow, if the data, used for Adam's steps is similar [26]. To overcome this issue the batches for Adam are made from randomly selected data points from the training subset.

Each of the NN was trained using a modified early-stopping regularization technique, described in Section 1.5.3. We don't stop the training at the moment the validation error starts to worsen but wait for 5-20 epochs to see if the validation performance will enhance. In case there is no positive effect from waiting, we stop training and restore the model where validation error is the best.

The architectures were selected based on the average loss metric (minus Sharpe ratio) over the batches of the model, trained on Period B. There is no clear scientific motivation for this methodology of optimal architecture selection for both periods. The reason for the selection of this metric is the fact that the author started the research from Period B and decided to do experiments on Period A much later. An alternative is to use some aggregative statistics taking into account

the validation performance of architecture in both periods. But this approach also doesn't have any scientific justifications. That is why it was decided to use only period B for selecting the models.

3.2 Layers

This section will describe the layers used for building the architectures for NNs. The layers can be seen as Lego cubics for constructing the NN.

3.2.1 Markowitz layer

This is the most important block in our NNs implemented using cvxpylaers, for constructing a convex optimization layer in a differentiable way. It encapsulates the essence of Markowitz portfolio optimization within a neural network paradigm, integrating this optimization directly into the neural network architecture. Two types of Markowitz layers are implemented.

The first one takes as input both the NN representation of expected returns and the covariance matrix of the assets. In the thesis, all the NNs, which are using this type of optimization layer have in their name a suffix 'FullOpti'. The implementation is adoption of the NumericalMarkowitz layer from deepdow package[45], the cost function is motivated by [12] The optimization problem is formulated as follows, incorporating both expected returns and the modified risk term, which is adjusted by a scaling parameter γ , and a regularization term to control the complexity of the portfolio weights:

Maximize with respect to \mathbf{w} :

$$\text{Objective} = \mathbf{r}^T \mathbf{w} - \gamma \cdot \sum_i (\Sigma^{1/2} \mathbf{w})_i^2 - \alpha \|\mathbf{w}\|_2 \quad (25)$$

Subject to:

$$\begin{aligned} \sum_{i=1}^N w_i &= 1, \\ |w_i| &\leq \text{max_weight}, \quad \forall i = 1, \dots, N. \end{aligned}$$

Where:

- $\Sigma^{1/2}$ is the square root of the covariance matrix of asset returns, used to calculate the modified risk.
- \mathbf{r} represents the vector of expected returns for each asset. Is computed by the NN based on datapoint input to the NN.
- γ is a parameter that scales the contribution of the risk term, allowing for the adjustment of the risk aversion level of the optimization.
- α is a non-negative regularization parameter that penalizes the complexity of the portfolio, promoting diversification and stability in the portfolio weights.

α and λ are learnable parameters, that are found during the NN training phase and are independent from the input data point. While $\Sigma^{1/2}$ and \mathbf{r} are computed taking based on the input.

This formulation allows for the direct optimization of portfolio weights based on obtained representations of asset returns and covariances, while also considering the risk tolerance and preference for portfolio weight complexity. The tolerance and the preferences are learned by the NN to according to our goals, the goals are defined by the loss function (in our case the goal is to maximize Sharpe ratio)

Another type of Markowitz layer is the one that tends to minimize portfolio variance. In the thesis NNs, utilizing this kind of layer have the suffix 'MinVar'. First of all the desire to test this kind of optimization layer was motivated by the accepted efficiency of minimum variance portfolios [11][16]. Another reason is based on the tendency of complex NNs to overfit. As will be shown MinVar optimization layers require fewer parameters: they don't need expected returns, risk-aversion, or regularization factors. As a result, an NN, which is based on MinVar optimization, tends to have fewer layers. The optimization problem aims at minimizing the portfolio's variance, adjusted for the constraints on the portfolio weights. The problem is formulated as:

Minimize with respect to \mathbf{w} :

$$\text{Risk} = \sum_i (\Sigma^{1/2} \mathbf{w})_i^2 \quad (26)$$

Subject to:

$$\begin{aligned} \sum_{i=1}^N w_i &= 1, \\ |w_i| &\leq \text{max_weight}, \quad \forall i = 1, \dots, N. \end{aligned}$$

The use of

$$\sum_i (\Sigma^{1/2} \mathbf{w})_i^2 \quad (27)$$

instead of

$$\mathbf{w}^T \Sigma \mathbf{w} \quad (28)$$

must be explained. As was mentioned before the Expression 28 is not DPP, so the layer with a cost function including this expression can't be differentiated. That is why Expression 28 was exchanged with expression 27. But this is not a problem, because the expressions are equivalent:

To show the equivalence between $\sum_i (\Sigma^{1/2} \mathbf{w})_i^2$ and $\mathbf{w}^T \Sigma \mathbf{w}$, we start by considering the definition of $\Sigma^{1/2}$, the square root of the covariance matrix Σ , which satisfies $\Sigma^{1/2} \Sigma^{1/2} = \Sigma$. Given a portfolio weight vector \mathbf{w} , we examine the expression $\sum_i (\Sigma^{1/2} \mathbf{w})_i^2$:

$$\sum_i (\Sigma^{1/2} \mathbf{w})_i^2 = (\Sigma^{1/2} \mathbf{w})^T (\Sigma^{1/2} \mathbf{w})$$

Applying the property that $\Sigma = \Sigma^{1/2}\Sigma^{1/2}$, we can rewrite the portfolio variance $\mathbf{w}^T\Sigma\mathbf{w}$ as follows:

$$\begin{aligned}\mathbf{w}^T\Sigma\mathbf{w} &= \mathbf{w}^T(\Sigma^{1/2}\Sigma^{1/2})\mathbf{w} \\ &= (\Sigma^{1/2}\mathbf{w})^T(\Sigma^{1/2}\mathbf{w})\end{aligned}$$

This final expression, $(\Sigma^{1/2}\mathbf{w})^T(\Sigma^{1/2}\mathbf{w})$, represents the dot product of the vector $\Sigma^{1/2}\mathbf{w}$ with itself, which is precisely the sum of the squares of its elements, $\sum_i(\Sigma^{1/2}\mathbf{w})_i^2$.

Thus, it is proven that $\sum_i(\Sigma^{1/2}\mathbf{w})_i^2$ is equivalent to $\mathbf{w}^T\Sigma\mathbf{w}$, establishing the interchangeability of these expressions for calculating portfolio risk in the context of optimization.

Although only two types of Markowitz layers were implemented, the power of NNs combined with the flexibility of convex optimization allows us to easily extend the set of available Markowitz layers. For example, we can formulate the following optimization layer. Suppose the input to our NN is a vector of features \mathbf{x} . Suppose the subset of \mathbf{x} , \mathbf{x}^B , represents Warren Buffett's opinion about the sign of expected returns for the portfolio asset returns for the period in time ($x_i^B = 1$ if asset returns will grow, and -1 if the asset will decline). And the subset of \mathbf{x} , \mathbf{x}_c , represents the information about the current economic cycle obtained from World Bank reports. The FullOpti can be extended in the following way.

Maximize with respect to \mathbf{w} :

$$\text{Objective} = \mathbf{r}^T\mathbf{w} - \gamma(\mathbf{x}_c) \cdot \sum_i(\Sigma^{1/2}\mathbf{w})_i^2 - \alpha\|\mathbf{w}\|_2 \quad (29)$$

Subject to:

$$\begin{aligned}\sum_{i=1}^N w_i &= 1, \\ |w_i| &\leq \text{max_weight}, \quad \forall i = 1, \dots, N, \\ w_i \cdot x_i^B &\geq 0, \quad \forall i = 1, \dots, N.\end{aligned}$$

This formulation introduces a new constraint to ensure that the investment strategy aligns with Warren Buffett's expectations: the portfolio takes long positions in assets that Buffett predicts will have positive returns and short positions in those he expects to have negative returns. This is captured by the constraint $w_i \cdot x_i^B \geq 0$ for each asset i , where w_i is the weight of the asset in the portfolio, and x_i^B reflects Buffett's opinion on the asset's return sign. The dynamic risk-aversion factor $\gamma(\mathbf{x}_c)$ can be obtained inside NN for example using a dense layer. It will compute optimal risk aversion for the current macro situation.

Actually, the amount of possible extensions is infinite, and the power of this approach is that investment ideas of the NN's creator can be easily injected into the NN.

3.2.2 Covariance layer

This subsection will provide a high-level description of the methodology used. But all the computations are made using the code provided by [45].

This layer transforms an input "data" matrix (the result of the previous transformations made by NN) into a square root of covariance matrix optionally using a version of shrinkage technique, described in Equation ??, in such a way, that the ability of NN to differentiate is preserved.

The forward pass algorithm below depicts high-level pseudocode for the one pass through the layer.

Algorithm 3 Forward Pass for Square Roots of Covariance Matrices

Require: X : tensor of shape $(batch_size, n_samples, n_assets)$, representing a list of matrix representations learned by NN about future asset returns

Require: $shrunk$: Boolean, indicating if shrinkage is applied

Ensure: List of square roots of covariance matrices, each of shape (n_assets, n_assets)

- 1: Initialize an empty list $SqrtCovarianceList$ to store the square roots of the covariance matrices
 - 2: **for** each x_i in X **do**
 - 3: $covariance_matrix \leftarrow compute_cov_matrix(x_i, shrunk)$
 - 4: $matrix_sqrt \leftarrow compute_sqrt(covariance_matrix)$
 - 5: Append $matrix_sqrt$ to $SqrtCovarianceList$
 - 6: **end for**
 - 7: **return** $SqrtCovarianceList$
-

Below can find the algorithm for the computation of covariance matrix $compute_cov_matrix$. The algorithm is using predefined $shrinkage_coeff$. The value was taken from DeepDow's original code. Further investigation of the influence of $shrinkage_coeff$ on model performance is needed.

Algorithm 4 Compute Covariance Matrix with Optional Diagonal Shrinkage

Require: M : matrix of shape $(n_assets, n_samples)$, representing asset observations

Require: $shrunk$: Boolean, indicating if diagonal shrinkage is applied

- 1: Set $shrinkage_coeff = 0.5$
 - 2: Subtract the mean of each row from its corresponding elements in M to center the data
 - 3: Let C be the centered data matrix $\triangleright C.shape = (n_assets, n_samples)$
 - 4: Compute the sample covariance matrix S as:
 - 5: $S = \frac{1}{n_samples-1} C C^T$ \triangleright This is the formula for S
 - 6: **if** $shrunk$ is True **then**
 - 7: Extract the diagonal of S to form a diagonal matrix D
 - 8: Apply diagonal shrinkage: $S \leftarrow shrinkage_coeff \times S + (1 - shrinkage_coeff) \times D$
 - 9: **end if**
 - 10: **return** S \triangleright Return the covariance matrix, with optional shrinkage
-

Given a positive definite covariance matrix M , our goal is to compute its square root. The Singular Value Decomposition (SVD) of M provides a reliable method for this purpose. SVD decomposes M into three matrices: U , Σ , and V^T , where U and V are orthogonal matrices, and Σ is a diagonal matrix with the singular values of M . Due to the symmetry of M , we have the simplification $U = V$, which facilitates the computation of M 's square root.

The procedure commences with performing the SVD of M , leading to the extraction of the singular values encapsulated in Σ . Subsequently, a new diagonal matrix $\Sigma_{\sqrt{\cdot}}$ is formed by taking the square root of each singular value in Σ . The square root matrix $M_{\sqrt{\cdot}}$ is then reconstructed using $V \Sigma_{\sqrt{\cdot}} V^T$. This process ensures that squaring $M_{\sqrt{\cdot}}$ indeed reconstructs the original matrix M , affirming the precision of $M_{\sqrt{\cdot}}$ as the true square root of M , this can be prove in the following way:

$$M_{\sqrt{}} \times M_{\sqrt{}} = V \Sigma_{\sqrt{}} V^T \times V \Sigma_{\sqrt{}} V^T = V \Sigma_{\sqrt{}} (V^T V) \Sigma_{\sqrt{}} V^T = V \Sigma_{\sqrt{}}^2 V^T = V \Sigma V^T = M$$

This formulaic demonstration explicitly shows how $M_{\sqrt{}}$ squared reconstructs M , validating the approach.

Below is the high-level pseudocode elucidating the steps to compute $M_{\sqrt{}}$ for a symmetric and positive definite matrix M (*compute_sqrt*):

Algorithm 5 Compute Square Root of Positive Definite Matrix

Require: M : Positive definite matrix of shape (n_assets, n_assets)

Ensure: Square root of M , denoted as $M_{\sqrt{}}$, of the same shape

```

1: Decompose  $M$  using Singular Value Decomposition (SVD):  $M = U \Sigma V^T$ 
2: Initialize  $\Sigma_{\sqrt{}}$  as an empty diagonal matrix of the same dimension as  $\Sigma$ 
3: for each singular value  $\sigma_i$  in  $\Sigma$  do
4:   if  $\sigma_i$  is above a predefined threshold then
5:     Replace  $\sigma_i$  in  $\Sigma_{\sqrt{}}$  with its square root,  $\sqrt{\sigma_i}$ 
6:   else
7:     Set the corresponding value in  $\Sigma_{\sqrt{}}$  to 0
8:   end if
9: end for
10: Reconstruct the square root of  $M$ :  $M_{\sqrt{}} = V \Sigma_{\sqrt{}} V^T$ 
11: return  $M_{\sqrt{}}$ 

```

The line 7 of the algorithm is introduced to avoid numerical instability, which can be caused by the computation of the square root of a too-small number. The threshold is derived by multiplying the maximum singular value by the dimension of the matrix and the machine epsilon, a tiny number representing the smallest distinguishable difference for the given floating-point type. It also should be noted the *SVD* decomposition is computed using torch built-in function [41], guaranteeing that all the operations in the layer are differentiable.

As a proposition of further research, it would be interesting to test the effectiveness of the denoising technique described in Section ??, after replacing shrinkage by denoising in Algorithm 4.

3.2.3 Normalization Layer

In Section 2.1.2 the effect of the disproportionality of input features on optimization was shown. Although for training we are using Adam optimizer, bringing input features to the same scale is important [46]. In the thesis, it is the responsibility of the Normalization layer to perform this kind of scaling. The layer adjusts the input features so they have a standard distribution, typically with a mean of zero and a standard deviation of one. This adjustment is applied per feature across the inputs it receives, ensuring a consistent and normalized data distribution that feeds into subsequent layers.

In machine learning the common approach is to compute the mean and the standard deviation based on the training dataset. And normalize data manually. However, the problem with this approach is that it assumes that the features' statistics won't change. But our features are returns of financial assets, which can change over time. That is why the normalization responsibility was delegated to NN. The actual technique applied is Batch Normalization[27].

In the Batch Normalization layer, which operates along the feature dimension, the input data is normalized by subtracting the mean and dividing by the standard deviation, calculated separately for each feature dimension across the batch. During training, the layer computes the mean μ_i and standard deviation σ_i for each feature dimension i as follows:

$$\mu_i = \frac{1}{N} \sum_{j=1}^N x_{ji}, \quad \sigma_i^2 = \frac{1}{N} \sum_{j=1}^N (x_{ji} - \mu_i)^2, \quad \sigma_i = \sqrt{\sigma_i^2}$$

where N is the batch size and x_{ji} is the value of the i th feature of the j th sample in the batch. During inference, the layer uses running estimates of the mean and standard deviation, running_mean_i and running_var_i , which are updated during training as running averages of the batch statistics. The normalized values \hat{x}_{ji} are then scaled and shifted using learnable parameters γ_i and β_i , resulting in the output y_{ji} :

$$\hat{x}_{ji} = \frac{x_{ji} - \text{running_mean}_i}{\sqrt{\text{running_var}_i + \epsilon}}, \quad y_{ji} = \gamma_i \hat{x}_{ji} + \beta_i$$

where ϵ is a small constant added for numerical stability. This normalization and scaling process helps stabilize and accelerate the training of neural networks. Moreover, it was shown that under certain conditions the layer can make Dropout usage redundant [27]. The torch-based implementations of the layer are used in the thesis [1, 2].

3.3 Other layers

The following layers are also utilized:

1. Dense layer. The layer which implements the function from Equation 4.
2. Dropout layer. The layer from Section 1.5.4
3. RNN and LSTM layers. Recurrent layers implementing ideas from Section 1.4.
4. Convolutional layer. Implement ideas from Section 1.3

4 Architectures

In this section, the implemented architectures will be described. Note these are 'the best' (in terms of validation error) architectures, the author could find during the research.

In general, the implemented architectures can be summarized in two steps:

1. Based on the input, create new representations of the assets covariance matrix and expected returns.
2. Solve the optimization problem.

All the networks are implemented with a lookback parameter equal to 50, several assets equal to 5, and a horizon equal to 5. In the diagrams, showing the architectures it is assumed that the sample size is n , and the text in lines between elements shows the dimensions. Note that even if Optimization Layer, solves Problem 25, γ and α will not be shown in the diagrams, because both γ and α , although being learnable parameters, are properties of NN itself, and are not transmitted between layers.

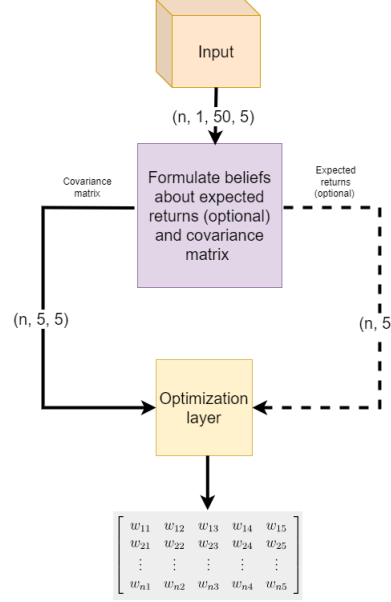


Рис. 19: General view on the implemented NNs.

The naming convention for implemented architectures is defined as follows:

Base format: {Major layer type name}Net{Suffix}

Suffix conditions: The suffix varies based on the problem being addressed:

- MinVar if Optimization layer is solving Problem 26.
- FullOpti if Problem 25 is solved.

5 DenseNet

DenseNet is a simple combination of dense layers with regularization dropout layers. Its architecture is shown in the image below. n represents the input sample size.

5.1 DenseNetFullOpti

The model architecture is shown in the figure below.

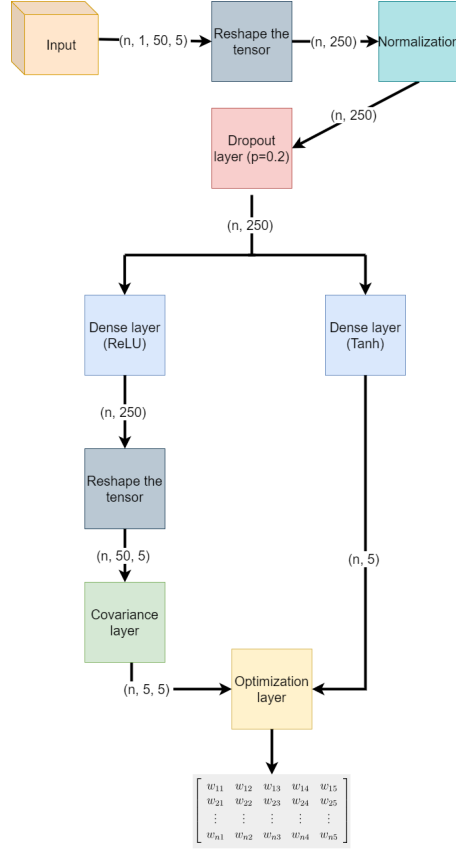


Рис. 20: DenseNetFullOpti architecture.

Several notes should be pointed out about the architecture:

1. Reshape is a differentiable operation. So it is legit to use it inside an NN.
2. Dropout should always be used after normalization because ignoring a fraction of data elements will definitely introduce bias into the normalization process.
3. As you can notice to compute the input into the Covariance Layer, and to compute expected returns Dense Layers are used. However, the activation functions differ. While for Covariance Layer input we can use almost any activation function, for computing of expected returns we can't use non-negative activations, such as ReLu. In the case of using ReLu, we will assume that negative returns are impossible, which is not true.

Figures below show the evolution of training and validation error through epochs for both training periods PeriodA and PeriodB. For this and the remaining NNs this kind of plot can be seen as proof that NNs learn new information from the data. The red line shows the stopping epoch. The epoch is selected based on the early stopping principles described in Section 1.5.

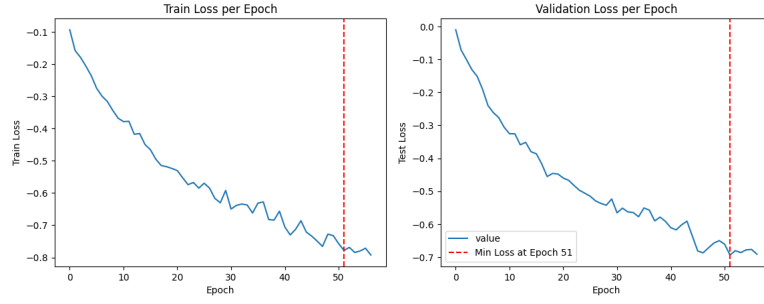


Рис. 21: DenseNetFullOpti training process (PeriodA).

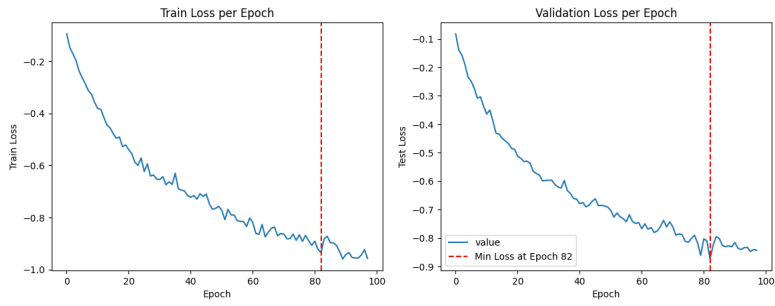


Рис. 22: DenseNetFullOpti training process (PeriodB).

5.2 DenseNetMinVar

The architecture is shown in the figure below.

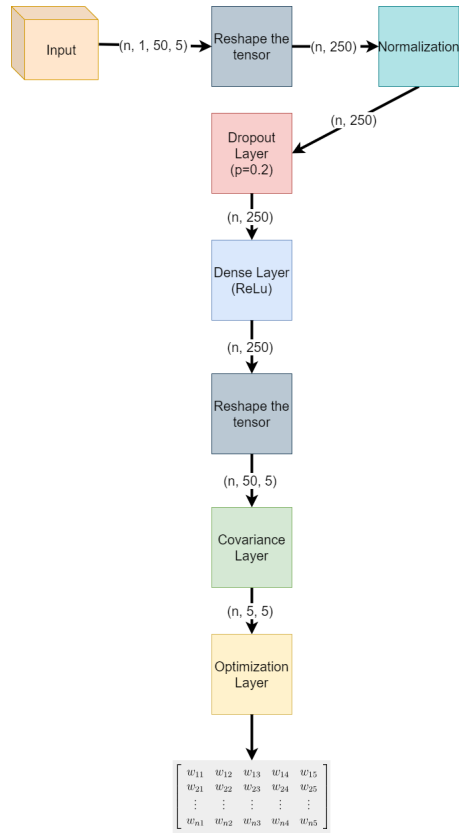


Рис. 23: DenseNetFullOpti architecture.

Below you can find the results for training for the models for both periods.

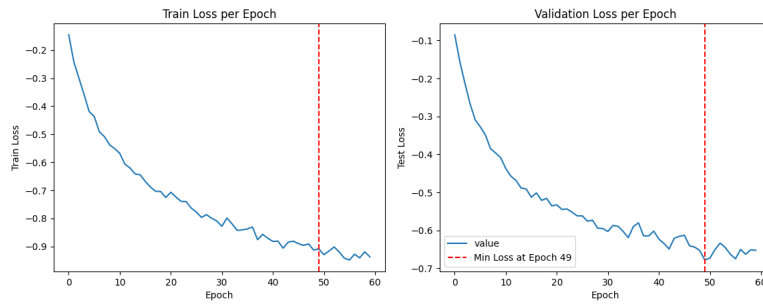


Рис. 24: DenseNetMinVar training process (PeriodA).

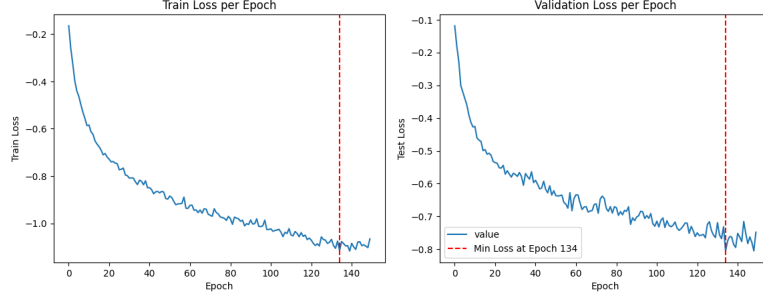


Рис. 25: DenseNetMinVar training process (PeriodB).

5.3 ConvNetNet

Convolutional layers are more often used for working with image data [32], but in our work, we construct a new representation from the matrix of daily asset returns. The applicability of the image-centered approach for financial returns is questionable. So actually in our work a modified version of the Equation 5 is used.

$$Y_{ij}^c = b_c + \sum_{m=1}^{H_f} K_m^c X_{i+m,j} \quad (30)$$

In the thesis, $H_f = 3$ is used. As a result Y_{ij}^C is a weighted average of three elements of the input plus bias. This is visualized in the figure below. The used Convolutional Layer passes through the matrix of asset returns, sequentially applying the filter (red rectangle).

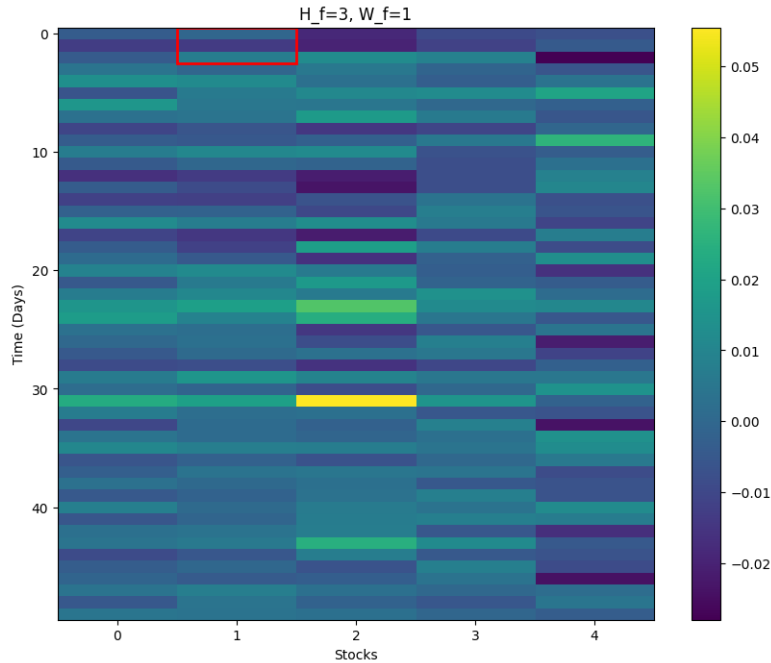


Рис. 26: $Y_{01}^c = b^1 + K_{00}^1 X_{01} + K_{10}^1 X_{11} + K_{20}^1 X_{21}$ (computer indexing used).

The motivation for this approach is the following: our input is a (H_{in}, W_{in}) matrix with H_{in} representing timesteps and W_{in} representing assets. While there is a certain order in the columns of the input matrix in the rows the order of returns is completely human-made. The author defined the order of assets while downloading the data. This is not the case for image data.

The figure below shows the importance of column positions for an image.

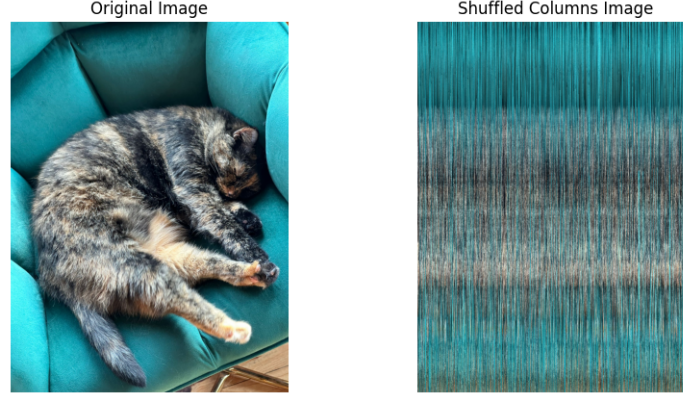


Рис. 27: The influence of columns shuffling on image data.

For asset returns, the original matrix is still informative after shuffling the columns even after removing the column names.

	Stock1	Stock2	Stock3
2024-01-01	-0.001353	0.014120	0.003198
2024-01-02	-0.001346	0.020830	-0.021771
2024-01-03	0.018512	-0.028073	0.002712
2024-01-04	0.028568	0.007888	0.007533
2024-01-05	0.007342	-0.027541	0.024717

	Stock3	Stock1	Stock2
2024-01-01	0.003198	-0.001353	0.014120
2024-01-02	-0.021771	-0.001346	0.020830
2024-01-03	0.002712	0.018512	-0.028073
2024-01-04	0.007533	0.028568	0.007888
2024-01-05	0.024717	0.007342	-0.027541

Рис. 28: The influence of columns shuffling on the stock returns matrix.

It can be claimed that for stock returns input the column's positions are not important, that is why horizontal neighbors of a stock, should be ignored during convolution.

As the reader will see later, each of the implemented architectures is using DenseLayer. The reason is the non-expressiveness of the original ConvLayer. The transformation made by the layer is too simple to learn something, without additional help.

5.3.1 ConvNetFullOpti

ConvNetFullOpti is a mix of dense and convolutional layers, utilizing both expected returns and covariance for portfolio optimization. After normalization, ConvNetFullOpti creates a two-channel representation of the input returns: expected returns channel and covariance channel. The obtained representations are used as input to the further layers.

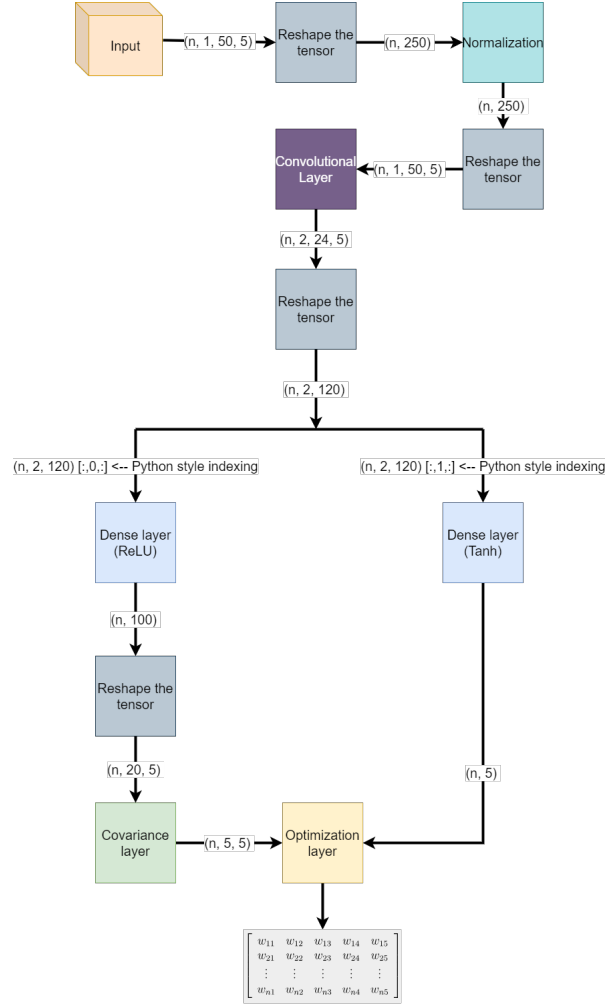


Рис. 29: ConvNetMinVar architecture.

The training process is shown below.

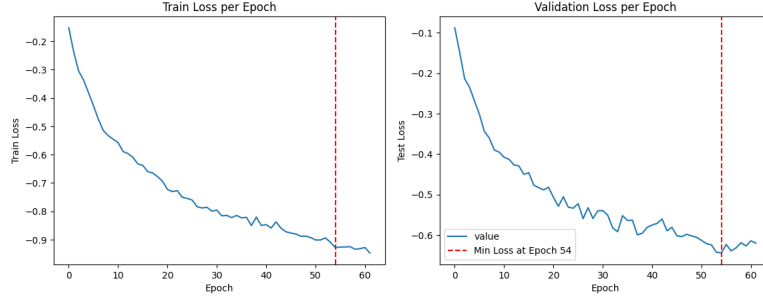


Рис. 30: ConvNetFullOpti architecture (PeriodA).

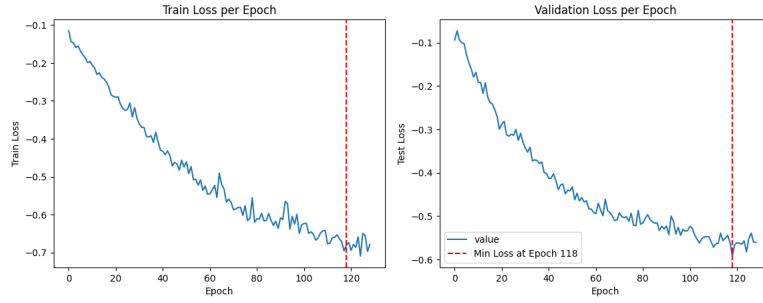


Рис. 31: ConvNetFullOpti architecture (PeriodB).

5.3.2 ConvNetMinVar

The idea of ConvNetMinVar is to learn a 3-channel representation of the original matrix, then aggregate it and use this aggregation as input for further modifications. The architecture is shown in the Figure below.

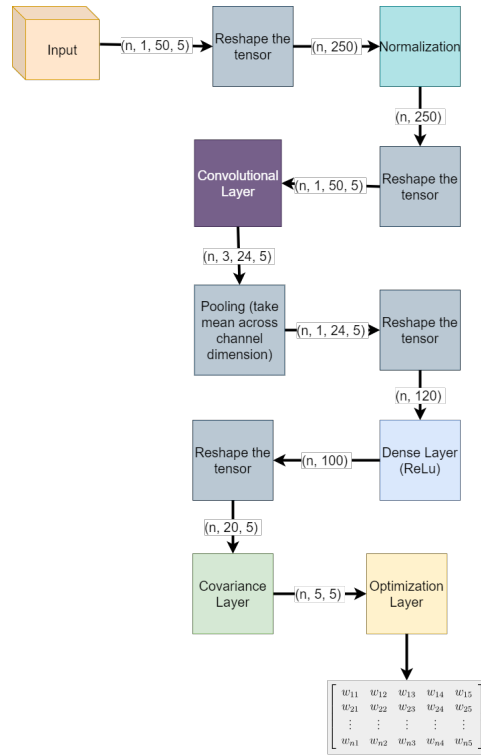


Рис. 32: ConvNetMinVar architecture.

The learning process of the built model is shown below.

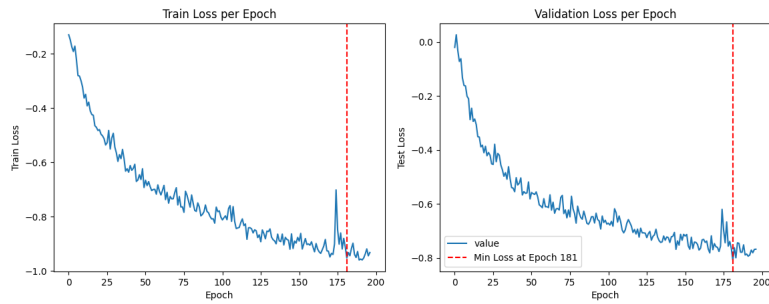


Рис. 33: ConvNetMinVar training process (PeriodA).

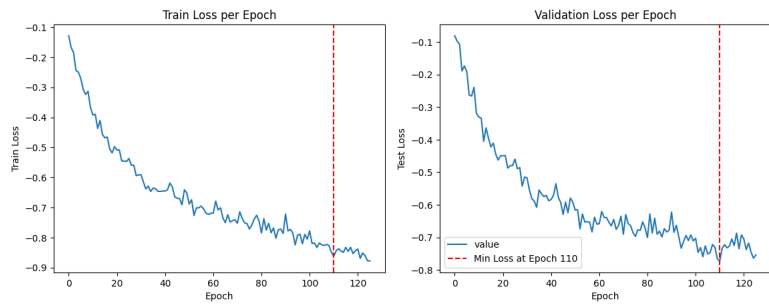


Рис. 34: ConvNetMinVar training process (PeriodB).

5.4 Recurrent architectures

In this subsection, both Recurrent Layer (RnnNet) and LSTM Layer (LstmNet) based architectures will be implemented. Note that the architectures are similar the only difference is in the recurrent layer used. The reason for the similar architecture is the fact that from the programmer's point of view, the interface of both RNN [3] and LSTM [40] are almost the same, and it is interesting to check if the LSTM complication of RNN will introduce some benefits to the NN.

5.5 Architectures

5.5.1 FullOpti

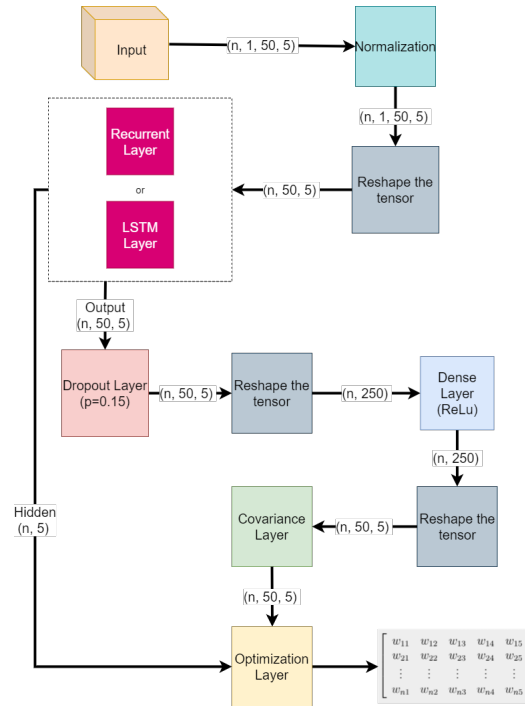


Рис. 35: recurrent network FullOpti architecture.

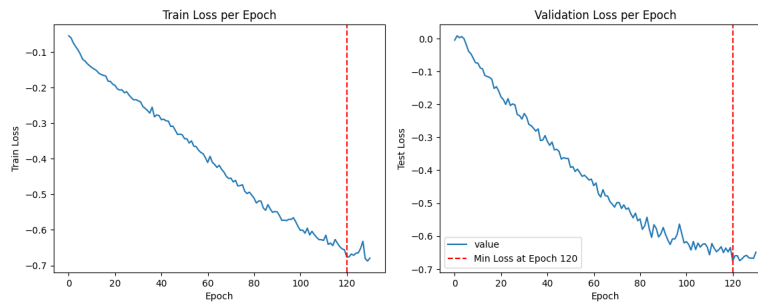


Рис. 36: RnnNetFullOpti training process (PeriodA).

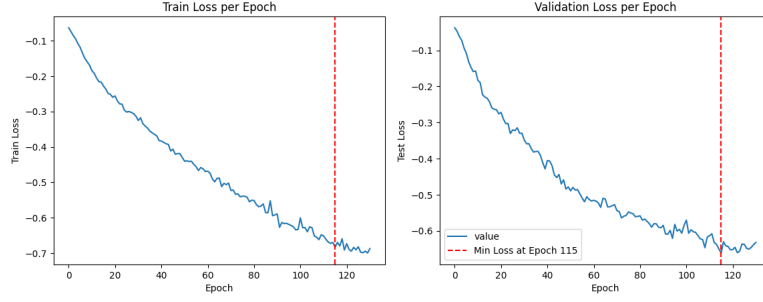


Рис. 37: RnnNetFullOpti training process (PeriodB).

5.5.2 MinVar

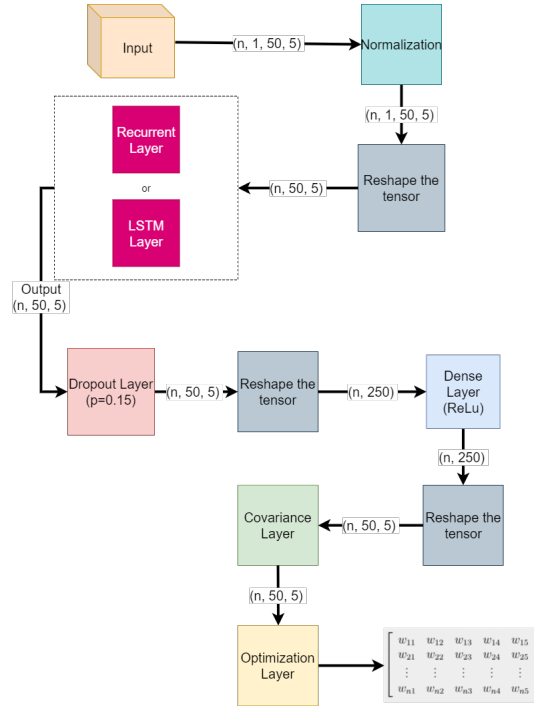


Рис. 38: recurrent network MinVar architecture.

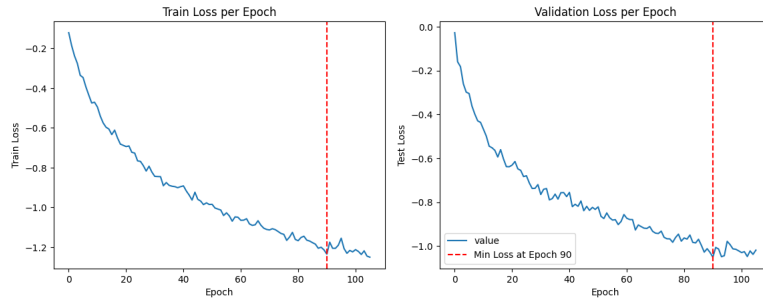


Рис. 39: RnnNetMinVar training process (PeriodA).

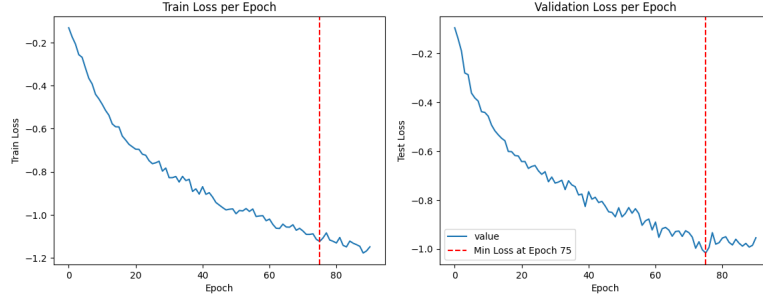


Рис. 40: RnnNetMinVar training process (PeriodB).

6 Experiments

The goal of our work is to compare the performance of classical algorithms and deep learning-based ones. To perform this comparison we will utilize backtesting. Backtesting is just running the rebalancing algorithm on specific data to gain an understanding of how the algorithm performs in general and how it generalizes on unseen market conditions (relevant for deep learning-based algorithms).

6.1 Data description

For this research, a strategic selection of five Exchange-Traded Funds (ETFs) was made to construct a diversified portfolio for backtesting. The chosen ETFs are: VWO (Vanguard FTSE Emerging Markets ETF), SPY (SPDR SP 500 ETF Trust), VNQ (Vanguard Real Estate ETF), LQD (iShares iBoxx \$ Investment Grade Corporate Bond ETF), and DBC (Invesco DB Commodity Index Tracking Fund). These ETFs were selected based on pivotal criteria:

- These ETFs belong to different asset classes;
- Uniform trading across all assets on the New York Stock Exchange to guarantee liquidity;
- Availability of comprehensive data for the designated training and testing periods.

Economic Rationality The selection is grounded on the economic rationale to support the diversification strategy:

- **VWO:** Provides exposure to a broad range of large and mid-sized companies in emerging markets, aiming for diversification across different economic conditions.
- **SPY:** Represents a wide swath of the U.S. equity market, capturing the performance of the SP 500.
- **VNQ:** Focuses on real estate investment trusts (REITs), reflecting the dynamics of the real estate sector.
- **LQD:** Comprises investment-grade corporate bonds, offering sensitivity to interest rate changes.
- **DBC:** Tracks a commodities index, subject to global economic trends and geopolitical events.

7 Experiment 1: Assessing NNs' Capability to Overfit Data

NNs have demonstrated substantial capabilities in memorizing complex datasets, which can lead to overfitting. This section evaluates the propensity of NNs to overfit using a specially configured DenseNetFullOpti model devoid of dropout mechanisms. This model is henceforth referred to as "Oracle."

7.1 Methodology

The experimental methodology is structured as follows:

1. Training the Oracle on the dataset for 200 epochs. The number of epochs used was selected based on the fact, that none of the trained NNs in Section 4, was trained for more than 200 epochs.
2. Conducting a backtest on the training period.

Experiments were conducted over two periods::

- period from December 15, 2020, to December 15, 2023;
- period from March 19, 2007, to December 15, 2023.

7.2 Period from December 15, 2020, to December 15, 2023

The Oracle achieved a cumulative return of 632.547% with a Sharpe Ratio of 2.86, outperforming the SPY and EWP portfolios for this period. SPY's Sharpe Ratio for the period is 0.56. Overall algorithm performance is shown in the figure below.

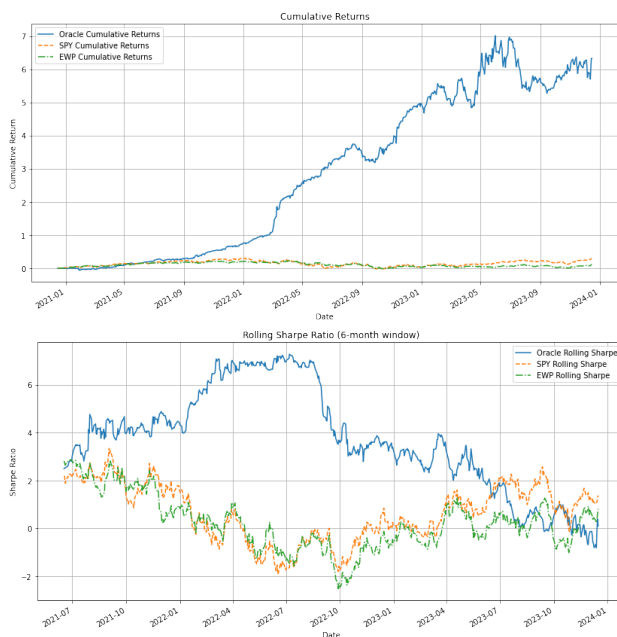


Рис. 41: Oracle vs SPY and EWP on seen data. Period form (2020-12-15) to (2023-12-15).

Key observations:

- There are periods when Oracle is losing money, besides seeing all the data. The source of the loss can be the fact that the algorithm is biased to long positions, due to the fact that the sum of portfolio weights should equal 1.
- There are periods when the rolling Sharpe Ratio of Oracle is lower than one of the others, despite Oracle being trained to maximize Sharpe Ratio. The reason can be the fact that Oracle was trained to maximize the Sharpe Ratio for the 7 days only.

7.3 Period from March 19, 2007, to December 15, 2023

During the backtest the algorithm returns -6631.369% cumulatively, with Sharpe Ratio -0.31 , performing much worse than SPY and EWP portfolios. While EWP cumulatively returned 49.407% for the period with a 0.23 Sharpe Ratio. Overall algorithm performance is shown in the figure below.

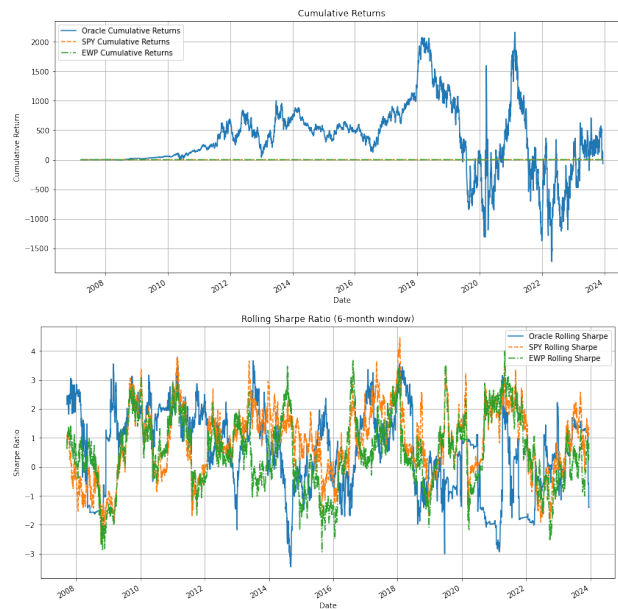


Рис. 42: Oracle vs SPY and EWP on seen data. Period from (2007-03-19) to (2023-12-15).

The following can be noted:

1. Besides seeing all the data, the algorithm was unable to remember the consequences of COVID and the Russian-Ukraine war. This can be explained by data imbalance. The majority of training data is from 'normal' market conditions, making it much harder for the algorithm to adapt to these events.
2. There are no long periods when the algorithm dominates SPY and EWP in terms of rolling Sharpe Ratio.

7.4 Conclusions and thoughts about the experiment

The summary of results above:

- The model performed well on the shorter period, besides not always being able to beat other portfolios in terms of rolling Sharpe Ratio, but overall performance is satisfactory.
- On the larger period shown an inability to deal with extreme events, and a tendency to follow the past trend.
- Based on cumulative returns dynamics, we can conclude that models can overfit (earning more than 2000% in certain points in time too good to be a coincidence).

It should be noted, that the author is sure, that the results above can easily be enhanced by increasing the number of epochs and usage of more complicated models.

The experiment can be repeated for the remaining seven implemented architectures, leading to the same conclusions.

8 Experiment 2: How the NNs will behave on unseen data

The experiment was carried out over two periods. This was done to show the vulnerability of the study to the backtest data selection process. The goal of the experiment is outlined in the title.

8.1 Period from January 3, 2017 to December 15, 2020

8.1.1 Experiment setup

The following facts characterize the period of training and backtesting timing:

- **Model Training Phase:** Models are trained on daily returns data of selected ETFs from January 3, 2007, to December 15, 2017. Based on this phase the model's architectures were selected, as was shown in Section ??.
- **Testing Phase:** The backtesting period extends from December 15, 2017, to December 15, 2020.
- **Annual Retraining:** All models are retrained annually on:
 - December 15, 2018;
 - December 15, 2019.

Below you can find the visualization of the timeline. Index prices are visualized to show the conditions under which the models were trained and backtested.

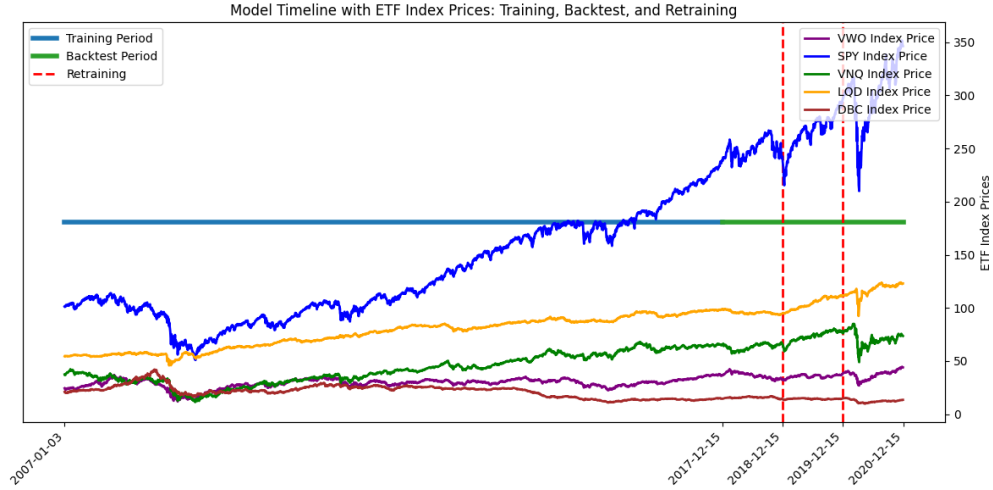


Рис. 43: Timeline of training and backtesting data (period from January 3, 2017 to December 15, 2020).

There are a lot of strategies to retrain NNs. One of the most popular approaches is to retrain an NN on all the available data by the time of retraining. For example, if the retraining is done on December 15, 2019, the retrained model is newly created and trained on all the available data (from January 3, 2007, to December 3, 2017). A popular alternative is to retrain the model only on the unseen data. Since we are retraining the models each year, the unseen data for a model is one-year data of daily returns. For example, if we are retraining a model on December 15, 2019, only data from December 15, 2018, to December 15, 2019, is used for retraining [13]. The problem with this approach is that one can easily destroy the results of the previous training and overfit to the new data (especially considering the small amount of data points in one year). That is why it was decided to retrain models on all the available data, despite this approach being much more computationally expensive.

The exception is retraining during the training phase. After the training process described in Section ??, the obtained trained model (you saw the figure of the training process for each model implemented in Section ??) was retrained on the validation set only to catch the relevant trends. To avoid overfitting to the validation set for retraining 25% of epochs of the original training process were used, moreover, the learning rate is 50% of the learning rate of the original. As an example suppose a model was trained for 80 epochs, with a learning rate of 0.001 on a tuning subset of a training set before it was stopped by early stopping. Then it will be retrained on the validation set for 20 epochs with a 0.0005 learning rate.

8.1.2 Experiment results

Таблица 1: Backtest Results without Transaction Costs: December 15, 2017, to December 15, 2020

Metrics	DenseNetMinVar	DenseNetFullOpti	ConvNetMinVar	ConvNetFullOpti	RnnNetMinVar		
Annual Return	5.31%	5.53%	6.07%	9.27%	0.78%		
Cumulative Returns	16.76%	17.50%	19.30%	30.42%	2.37%		
Annual Volatility	12.15%	16.62%	15.79%	15.02%	15.16%		
Sharpe Ratio	0.49	0.41	0.45	0.67	0.13		
Calmar Ratio	0.23	0.21	0.20	0.49	0.02		
Stability	0.59	0.36	0.42	0.68	0.04		
Max Drawdown	-23.58%	-26.43%	-30.35%	-18.94%	-34.25%		
Omega Ratio	1.11	1.1	1.1	1.13	1.03		
Sortino Ratio	0.66	0.53	0.64	0.92	0.17		
VaR (97.5%)	-1.51%	-2.07%	-1.96%	-1.85%	-1.90%		
ES (97.5%)	-0.02717	-0.03975	-0.03338	-0.03052	0.03230		
Interweight Distance	0.06865	0.16567	0.14634	0.09492	0.14590		

Metrics	RnnNetFullOpti	LstmNetMinVar	LsmNetFullOpti	MinVar	FullOpti	EWP	SPY
Annual Return	2.43%	1.07%	-1.10%	2.80%	3.06%	3.73%	11.42%
Cumulative Returns	7.46%	3.22%	-3.27%	8.62%	9.46%	11.59%	38.27%
Annual Volatility	16.02%	15.19%	16.67%	9.85%	15.60%	16.23%	22.92%
Sharpe Ratio	0.23	0.15	0.02	0.33	0.27	0.31	0.59
Calmar Ratio	0.09	0.04	-0.04	0.15	0.10	0.12	0.33
Stability	0.48	0.02	0	0.52	0	0.02	0.56
Max Drawdown	-27.47%	-25.23%	-27.18%	-18.07%	-29.48%	-30.00%	-34.10%
Omega Ratio	1.06	1.03	1	1.08	1.06	1.07	1.13
Sortino Ratio	0.31	0.19	0.02	0.47	0.35	0.40	0.80
VaR (97.5%)	-2.00%	-1.90%	-2.10%	-1.23%	-1.95%	-2.03%	-2.83%
ES (97.5%)	-0.03624	-0.03378	-0.03917	-0.02103	-0.03495	-0.03615	-0.04831
Interweight Distance	0.15993	0.13608	0.11833	0.01648	0.00882	0	0

Таблица 2: Backtest Results with Transaction Costs (C=0.01% per dollar): December 15, 2017, to December 15, 2020

Metrics	DenseNetMinVar	DenseNetFullOpti	ConvNetMinVar	ConvNetFullOpti	RnnNetMinVar
Annual Return	1.98%	-2.80%	-0.93%	4.29%	-5.92%
Cumulative Returns	6.04%	-8.14%	-2.77%	13.41%	-16.71%
Annual Volatility	12.17%	16.62%	15.81%	15.04%	15.13%
Sharpe Ratio	0.22	-0.09	0.02	0.35	-0.33
Calmar Ratio	0.08	-0.09	-0.03	0.21	-0.14
Stability	0.2	0.15	0.13	0.3	0.55
Max Drawdown	-23.88%	-32.80%	-33.70%	-20.89%	-43.16%
Omega Ratio	1.05	0.98	1	1.07	0.93
Sortino Ratio	0.3	-0.11	0.03	0.49	-0.43
VaR (97.5%)	-1.52%	-2.10%	-1.99%	-1.87%	-1.93%
ES (97.5%)	-0.02731	-0.03966	-0.03347	-0.03054	-0.03224
Interweight Distance	0.06865	0.16567	0.14634	0.09492	0.14590

Metrics	RnnNetFullOpti	LstmNetMinVar	LsmNetFullOpti	MinVar	FullOpti	EWP	SPY
Annual Return	-3.98%	-5.00%	-5.88%	1.97%	2.65%	3.73%	11.42%
Cumulative Returns	-11.45%	-14.23%	-16.60%	6.01%	8.14%	11.59%	38.27%
Annual Volatility	16.01%	15.22%	16.65%	9.87%	15.60%	16.23%	22.92%
Sharpe Ratio	-0.17	-0.26	-0.28	0.25	0.25	0.31	0.59
Calmar Ratio	-0.13	-0.16	-0.18	0.11	0.09	0.12	0.33
Stability	0.10	0.53	0.45	0.42	0	0.02	0.56
Max Drawdown	-31.60%	-30.61%	-32.95%	-18.26%	-29.55%	-30.00%	-34.10%
Omega Ratio	0.96	0.94	0.94	1.06	1.05	1.07	1.13
Sortino Ratio	-0.23	-0.33	-0.37	0.35	0.32	0.40	0.80
VaR (97.5%)	-2.03%	-1.93%	-2.12%	-1.23%	-1.95%	-2.03%	-2.83%
ES (97.5%)	-0.03610	-0.03392	-0.03919	-0.02114	-0.03496	-0.03615	-0.04831
Interweight Distance	0.15993	0.13608	0.11833	0.01648	0.00882	0	0

8.1.3 Key Observations

- All the non-recurrent NNs show good results without transaction costs. ConvNetFullOpti was even able to beat SPY in terms of the Sharpe Ratio.
- Transaction costs destroyed, almost advantage. None of the models was even able to beat EWP.
- Bad performance of the recurrent networks looks strange. Theoretically, these are the most appropriate models to work with time series data.

8.2 Period from January 01, 2007 to December 15, 2023

8.2.1 Experiment setup

- **Model Training Phase:** Models are trained on daily returns data of selected ETFs from January 3, 2007, to December 15, 2020. As for the previous, models architectures are selected during this phase.

- **Testing Phase:** The backtesting period extends from December 15, 2020, to December 15, 2023.
- **Annual Retraining:** All models are retrained annually on:
 - December 15, 2021
 - December 15, 2022

Below you can find the visualization of the timeline.

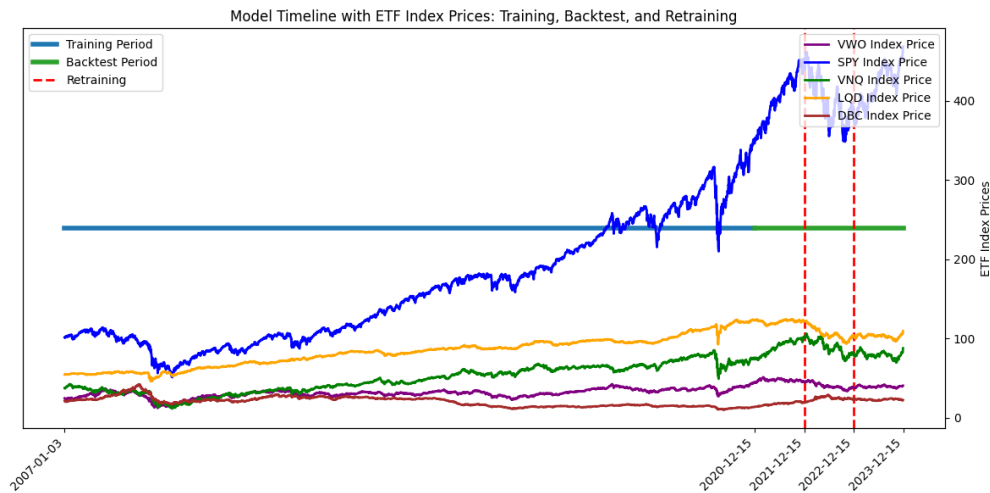


Рис. 44: Timeline of training and backtesting data (period from January 01, 2007 to December 15, 2023).

8.2.2 Experiment results

Таблица 3: Backtest Results without Transaction Costs: December 15, 2020, to December 15, 2023

Metrics	DenseNetMinVar	DenseNetFullOpti	ConvNetMinVar	ConvNetFullOpti	RnnNetMinVar
Annual Return	0.39%	-3.84%	3.48%	-3.44%	-5.73%
Cumulative Returns	1.17%	-11.12%	10.85%	-9.98%	-16.27%
Annual Volatility	10.50%	12.94%	13.65%	13.31%	12.08%
Sharpe Ratio	0.09	-0.24	0.32	-0.20	-0.43
Calmar Ratio	0.02	-0.13	0.17	-0.11	-0.20
Stability	0.36	0.67	0.01	0.53	0.80
Max Drawdown	-19.25%	-29.43%	-19.98%	-30.15%	-28.58%
Omega Ratio	1.02	0.96	1.06	0.97	0.93
Sortino Ratio	0.13	-0.34	0.46	-0.27	-0.59
VaR (97.5%)	-1.32%	-1.64%	-1.70%	-1.69%	-1.54%
ES (97.5%)	-0.01794	-0.02110	-0.02236	-0.02251	-0.02113
Interweight Distance	0.07005	0.15172	0.14457	0.13020	0.13375

Metrics	RnnNetFullOpti	LstmNetMinVar	LsmNetFullOpti	MinVar	FullOpti	EWP	SPY
Annual Return	-11.35%	-2.64%	1.03%	-7.33%	3.59%	3.46%	8.68%
Cumulative Returns	-30.40%	-7.74%	3.13%	-20.46%	11.19%	10.77%	28.46%
Annual Volatility	15.09%	12.52%	12.09%	9.04%	12.74%	12.38%	17.59%
Sharpe Ratio	-0.72	-0.15	0.15	-0.80	0.34	0.34	0.56
Calmar Ratio	-0.24	-0.08	0.04	-0.26	0.18	0.17	0.34
Stability	0.84	0.72	0.34	0.82	0.23	0.18	0.02
Max Drawdown	-48.07%	-31.56%	-25.49%	-28.07%	-20.20%	-20.22%	-25.36%
Omega Ratio	0.88	0.97	1.03	0.87	1.06	1.06	1.10
Sortino Ratio	-0.95	-0.21	0.21	-1.07	0.48	0.48	0.80
VaR (97.5%)	-1.95%	-1.59%	-1.52%	-1.17%	-1.59%	-1.54%	-2.18%
ES (97.5%)	-0.02943	-0.02213	-0.02046	-0.01592	-0.02245	-0.02027	-0.03060
Interweight Distance	0.18034	0.12900	0.11459	0.02055	0.00908	0.00	0.00

Backtest Results with Transaction Costs: December 15, 2020, to December 15, 2023

Metrics	DenseNetMinVar	DenseNetFullOpti	ConvNetMinVar	ConvNetFullOpti	RnnNetMinVar
Annual Return	-2.98%	-10.53%	-3.52%	-9.14%	-11.70%
Cumulative Returns	-8.69%	-28.44%	-10.21%	-25.04%	-31.23%
Annual Volatility	10.52%	13.11%	13.76%	13.37%	12.14%
Sharpe Ratio	-0.23	-0.78	-0.19	-0.65	-0.96
Calmar Ratio	-0.13	-0.28	-0.14	-0.26	-0.30
Stability	0.69	0.86	0.57	0.78	0.91
Max Drawdown	-22.22%	-37.13%	-24.27%	-34.94%	-38.89%
Omega Ratio	0.96	0.88	0.97	0.90	0.85
Sortino Ratio	-0.33	-1.08	-0.27	-0.88	-1.30
VaR (97.5%)	-1.34%	-1.69%	-1.74%	-1.72%	-1.58%
ES (97.5%)	-0.01806	-0.02151	-0.02274	-0.02285	-0.02126
Interweight Distance	0.07005	0.15172	0.14457	0.13020	0.13375

Metrics	RnnNetFullOpti	LstmNetMinVar	LsmNetFullOpti	MinVar	FullOpti	EWP	SPY
Annual Return	-18.54%	-8.44%	-4.21%	-8.26%	3.16%	3.46%	8.68%
Cumulative Returns	-46.02%	-23.30%	-12.14%	-22.83%	9.82%	10.77%	28.46%
Annual Volatility	15.18%	12.59%	12.13%	9.04%	12.75%	12.38%	17.59%
Sharpe Ratio	-1.27	-0.64	-0.29	-0.91	0.31	0.34	0.56
Calmar Ratio	-0.32	-0.22	-0.13	-0.29	0.15	0.17	0.34
Stability	0.90	0.86	0.70	0.84	0.27	0.18	0.02
Max Drawdown	-57.38%	-38.97%	-31.27%	-28.87%	-20.49%	-20.22%	-25.36%
Omega Ratio	0.80	0.89	0.95	0.86	1.05	1.06	1.10
Sortino Ratio	-1.65	-0.88	-0.41	1.22	0.43	0.48	0.80
VaR (97.5%)	-1.99%	-1.62%	-1.54%	-1.17%	-1.59%	-1.54%	-2.18%
ES (97.5%)	-0.02980	-0.02246	-0.02073	-0.01594	-0.02246	-0.02027	-0.03060
Interweight Distance	0.18034	0.12900	0.11459	0.02055	0.00908	0.00	0.00

8.2.3 Key Observations

None of the NN-based models was able to outperform EWP without transaction costs during the period. That is why it was decided not to show the results with transaction costs. This can be explained using the example of LstmFullOpti:

1. The model has acceptable performance (in terms of rolling Sharpe Ratio shown in Figure below) when the market is growing because it was trained on bullish as shown in Figure 8.2.3.
2. But when the market conditions are changing starting from 2022 the model's knowledge about the market is becoming.
3. Due to the retraining structure the model is retrained taking into the very pessimistic period from December 15, 2022, to December 15, 2023. Due to this pessimistic bias, it is unable to show good performance, when the market starts growing again.

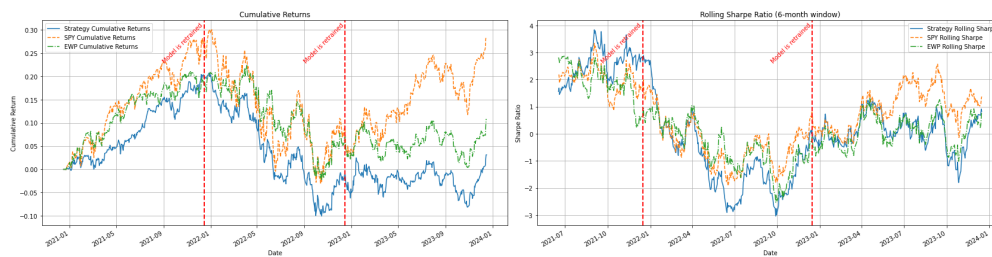


Рис. 45: LstmFullOpti backtest results (period period from December 15, 2020, to December 15, 2023).

Список литературы

- [1] torch.nn.batchnorm1d. <https://pytorch.org/docs/stable/generated/torch.nn.BatchNorm1d.html>. Accessed: April 8, 2024.
- [2] torch.nn.batchnorm2d. <https://pytorch.org/docs/stable/generated/torch.nn.BatchNorm2d.html>. Accessed: April 8, 2024.
- [3] torch.nn.RNN – pytorch 1.x documentation. <https://pytorch.org/docs/stable/generated/torch.nn.RNN.html>, 2024.

- [4] A. Agrawal, B. Amos, S. Barratt, S. Boyd, S. Diamond, and J. Z. Kolter. Differentiable convex optimization layers. *Advances in neural information processing systems*, 32, 2019.
- [5] A. Agrawal, R. Verschueren, S. Diamond, and S. Boyd. A rewriting system for convex optimization problems. *Journal of Control and Decision*, 5(1):42–60, 2018.
- [6] D. Anguita, L. Ghelardoni, A. Ghio, L. Oneto, S. Ridella, et al. The k’in k-fold cross validation. In *ESANN*, volume 102, pages 441–446, 2012.
- [7] anucvml. Eeccv2020 tutorial - differentiable optimization layers - basic concepts. YouTube, 2020. Available at <https://youtu.be/oCDtHwU4KY>.
- [8] C. authors. Disciplined convex programming. CVXPY Documentation, 2024. Available at <https://www.cvxpy.org/tutorial/dcp/index.html>.
- [9] C. Banerjee, T. Mukherjee, and E. Pasiliao Jr. An empirical study on generalizations of the relu activation function. In *Proceedings of the 2019 ACM Southeast Conference*, pages 164–167, 2019.
- [10] bayerj (<https://stats.stackexchange.com/users/2860/bayerj>). How does lstm prevent the vanishing gradient problem? Cross Validated. URL:<https://stats.stackexchange.com/q/263956> (version: 2017-12-30).
- [11] Z. Bednarek and P. Patel. Understanding the outperformance of the minimum variance portfolio. *Finance Research Letters*, 24:175–178, 2018.
- [12] T. Bodnar, N. Parolya, and W. Schmid. On the equivalence of quadratic optimization problems commonly used in portfolio theory. *European Journal of Operational Research*, 229(3):637–644, 2013.
- [13] J. Brownlee. How to update your neural network models with more data. <https://machinelearningmastery.com/update-neural-network-models-with-more-data/>, 2017. Accessed: 2024-04-14.
- [14] A. Choromanska, M. Henaff, M. Mathieu, G. B. Arous, and Y. LeCun. The loss surfaces of multilayer networks. In *Artificial intelligence and statistics*, pages 192–204. PMLR, 2015.
- [15] CVXPY Developers. Advanced Features — CVXPY 1.4 documentation. <https://www.cvxpy.org/tutorial/advanced/index.html>, 2023. Accessed: 2024-04-10.
- [16] R. L. De Carvalho, X. Lu, and P. Moulin. Demystifying equity risk-based strategies: A simple alpha plus beta description. *The Journal of Portfolio Management*, 38(3):56–70, 2012.
- [17] S. Diamond and S. Boyd. Cvxpy: A python-embedded modeling language for convex optimization. *The Journal of Machine Learning Research*, 17(1):2909–2913, 2016.
- [18] K. Fukushima. Neocognitron: A self-organizing neural network model for a mechanism of pattern recognition unaffected by shift in position. *Biological cybernetics*, 36(4):193–202, 1980.
- [19] G. Goh. Why momentum really works. *Distill*, April 2017.
- [20] D. Goldberg. What every computer scientist should know about floating-point arithmetic. *ACM computing surveys (CSUR)*, 23(1):5–48, 1991.
- [21] I. Goodfellow, Y. Bengio, and A. Courville. *Deep Learning*. MIT Press, 2016. <http://www.deeplearningbook.org>.
- [22] I. Goodfellow, D. Warde-Farley, M. Mirza, A. Courville, and Y. Bengio. Maxout networks. In *International conference on machine learning*, pages 1319–1327. PMLR, 2013.
- [23] S. Hochreiter and J. Schmidhuber. Long short-term memory. *Neural computation*, 9(8):1735–1780, 1997.
- [24] K. Hornik, M. Stinchcombe, and H. White. Universal approximation of an unknown mapping and its derivatives using multilayer feedforward networks. *Neural networks*, 3(5):551–560, 1990.
- [25] T. (<https://stats.stackexchange.com/users/56984/tim>). What are the differences between 39;epoch39;, 39;batch39;, and 39;minibatch39;? Cross Validated. URL:<https://stats.stackexchange.com/q/117919> (version: 2021-02-17).

- [26] J. (https://stats.stackexchange.com/users/89653/josh). Why should we shuffle data while training a neural network? Cross Validated. URL:https://stats.stackexchange.com/q/311318 (version: 2017-11-09).
- [27] S. Ioffe and C. Szegedy. Batch normalization: Accelerating deep network training by reducing internal covariate shift. In *International conference on machine learning*, pages 448–456. pmlr, 2015.
- [28] D. P. Kingma and J. Ba. Adam: A method for stochastic optimization. *arXiv preprint arXiv:1412.6980*, 2014.
- [29] Y. LeCun. Training with large minibatches is bad for your health. more importantly, it’s bad for your test error. friends don’t let friends use minibatches larger than 32. Twitter, 2018. Tweet.
- [30] M. Leshno, V. Y. Lin, A. Pinkus, and S. Schocken. Multilayer feedforward networks with a nonpolynomial activation function can approximate any function. *Neural networks*, 6(6):861–867, 1993.
- [31] Z. C. Lipton, J. Berkowitz, and C. Elkan. A critical review of recurrent neural networks for sequence learning. *arXiv preprint arXiv:1506.00019*, 2015.
- [32] L. Ma, Z. Lu, and H. Li. Learning to answer questions from image using convolutional neural network. In *Proceedings of the AAAI Conference on Artificial Intelligence*, volume 30, 2016.
- [33] A. L. Maas, A. Y. Hannun, A. Y. Ng, et al. Rectifier nonlinearities improve neural network, acoustic models. In *Proc. icml*, volume 30, page 3. Atlanta, GA, 2013.
- [34] P. Nakkiran, G. Kaplun, Y. Bansal, T. Yang, B. Barak, and I. Sutskever. Deep double descent: Where bigger models and more data hurt. *Journal of Statistical Mechanics: Theory and Experiment*, 2021(12):124003, 2021.
- [35] Y. Nesterov and A. Nemirovsky. Conic formulation of a convex programming problem and duality. *Optimization Methods and Software*, 1(2):95–115, 1992.
- [36] M. A. Nielsen. *Neural networks and deep learning*, volume 25. Determination press San Francisco, CA, USA, 2015.
- [37] T. Nitta. Solving the xor problem and the detection of symmetry using a single complex-valued neuron. *Neural Networks*, 16(8):1101–1105, 2003.
- [38] P. Patrinos. Optimization lecture notes. <https://www.kuleuven.be/english>, 2023. Lecture Notes for Course on Optimization.
- [39] D. S. Poskitt. A note on autoregressive modeling. *Econometric Theory*, 10(5):884–899, 1994.
- [40] PyTorch. torch.nn.lstm - pytorch documentation. <https://pytorch.org/docs/stable/generated/torch.nn.LSTM.html>, 2023. Accessed: 2024-03-25.
- [41] PyTorch. torch.svd - pytorch documentation. <https://pytorch.org/docs/stable/generated/torch.svd.html>, 2023. Accessed: 2023-04-04.
- [42] S. Raschka. *Python machine learning*. Packt publishing ltd, 2015.
- [43] S. J. Reddi, S. Kale, and S. Kumar. On the convergence of adam and beyond. *arXiv preprint arXiv:1904.09237*, 2019.
- [44] D. Rolnick, A. Veit, S. Belongie, and N. Shavit. Deep learning is robust to massive label noise. *arXiv preprint arXiv:1705.10694*, 2017.
- [45] J. Siebert, J. Groß, and C. Schroth. A systematic review of python packages for time series analysis. *arXiv preprint arXiv:2104.07406*, 2021.
- [46] J. Sola and J. Sevilla. Importance of input data normalization for the application of neural networks to complex industrial problems. *IEEE Transactions on nuclear science*, 44(3):1464–1468, 1997.
- [47] N. Srivastava, G. Hinton, A. Krizhevsky, I. Sutskever, and R. Salakhutdinov. Dropout: a simple way to prevent neural networks from overfitting. *The journal of machine learning research*, 15(1):1929–1958, 2014.

- [48] T. Tieleman. Lecture 6.5-rmsprop: Divide the gradient by a running average of its recent magnitude. *COURSERA: Neural networks for machine learning*, 4(2):26, 2012.
- [49] C. University. Lecture 7: Advanced topics in machine learning and data science. <https://www.cs.cornell.edu/courses/cs6787/2017fa/Lecture7.pdf>, 2017. Accessed: 2024-04-02.
- [50] C. University. Stochastic gradient descent. https://optimization.cbe.cornell.edu/index.php?title=Stochastic_gradient_descent, 2024. Accessed: 2024-04-02.
- [51] R. Zadeh. The hard thing about deep learning. <https://www.oreilly.com/radar/the-hard-thing-about-deep-learning/>, 11 2016. Accessed: 2024-04-02.
- [52] A. Zhang, Z. C. Lipton, M. Li, and A. J. Smola. Dive into deep learning, 2021. Online; accessed February 26, 2024.
- [53] C. Zhang, S. Bengio, M. Hardt, B. Recht, and O. Vinyals. Understanding deep learning (still) requires rethinking generalization. *Communications of the ACM*, 64(3):107–115, 2021.
- [54] Z. Zhang, S. Zohren, and S. Roberts. Deep learning for portfolio optimization. *The Journal of Financial Data Science*, 2020.